UNIVERSITY OF TURKISH AERODYNAMIC ASSOCIATION

AERONAUTICS AND ASTRONAUTICS

NUMERICAL INVESTIGATION ON HYDROTHERMAL PERFORMANCE OF A HELICAL ANNULAR TURBULENT FLOW IN HEAT EXCHANRER

MASTER THESIS

TAWFEEQ NAJI HUSSEIN

ID: 1403730062

Institute of Science and Technology

Mechanical and Aeronautical Engineering Department

Master Thesis Program

June, 2017

UNIVERSITY OF TURKISH AERODYNAMIC ASSOCIATION

AERONAUTICS AND ASTRONAUTICS

MASTER THESIS

TAWFEEQ NAJI HUSSEIN

ID: 1403730062

Re. NO: 10153322

NUMERICAL INVESTIGATION ON HYDROTHERMAL PERFORMANCE OF A HELICAL ANNULAR TURBULENT FLOW IN HEAT EXCHANGER

Supervisor: Assist. Prof. Dr. Munir ElFarra

CO. Supervisor: Dr. Kadhim Fadhil Nasir

بسم الله الرحمن الرحيم

الله لا اله الا هو الحي القيوم لا تأخذه سنه ولا نوم له ما في السموات وما في الأرض من ذا الذي يشفع عنده الا بأذنه يعلم ما بين ايديهم وما خلفهم ولا يحيطون بشيء من علمه الا بما شاء الله وسع كرسيه السموات والارض ولا يؤده حفظهما وهو العلي العظيم.

(صدق الله العلي العظيم)

Türk Hava Kurumu Üniversitesi Fen Bilimleri Enstitüsü'nün 1403730062 numaralı Yüksek Lisans öğrencisi "Tawfeeq Naji" ilgili yönetmeliklerin belirlediği gerekli tüm şartları yerine getirdikten sonra hazırladığı "Numerical investigation on hydrothermal performance of a helical annular turbulent flow in heat exchanger

" başlıklı tezini, aşağıda imzaları bulunan jüri önünde başarı ile sunmuştur.

Tez Danışmanı   : Yrd. Doç. Dr. Munir Elfarra
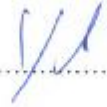   Ankara Yıldırım Beyazit Üniversitesi

Jüri Üyeleri   : Yrd. Doç. Dr. Durmuş Sinan Körpe
                       Türk Hava Kurumu Üniversitesi

                       : Yrd. Doç. Dr. Mohamed S. Elmnefi
                       Türk Hava Kurumu Üniversitesi

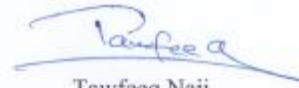   : Yrd. Doç. Dr. Munir Elfarra
                       Ankara Yıldırım Beyazit Üniversitesi

Tez Savunma Tarihi: 14.06.2017

i

STATEMENT OF NON-PLAGIARISM PAGE

I hereby declare that all information in this document has been obtained and presented in accordance with academic rules and ethical conduct. I also declare that, as required by these rules and conduct, I have fully cited and referenced all material and results that are not original to this work.

Tawfeeq Naji

14.06.2017

Acknowledgements

I would like to express my sincere gratitude to Dr. Asst .Pro . Miner Ali, my director, for her direction supervision, and sharing of expertise which guided me through my research period. I would also like to thank Dean Technical Institute Musayyib D. Asst. Jabber Abbas Japer . His supports and thoughtful advices to my research work

I am sincerely and heartily acknowledge my colleagues, advice relating to my research that they gave me. In the same way, I appreciate all the help and support from my friends me throughout my study.

Finally, I would like to express my deepest gratitude to all my family members: my father and mother my brother and sister, who constantly provided their emotional support to me during my research years. my wife, deserves special thanks for her caring of our family during these years. Your encouragement and support without regrets get me through those difficult times. Nobody knows how much I owe them.

And last but not least, a heartfelt thanks to all my flat mates for the great time spent together. It has been a wonderful experience!

June 2017   Tawfeeq Najı

Contents

List of Tables

List of figures

Abstract

Numerical investigation on hydrothermal performance of a helical annular turbulent flow in heat exchanger

TAWFEEQ NAJI HUSSEIN

Master. Department of Aeronautics and Mechanical Engineering

Supervisor: Assist. Prof. Dr. Munir Elfarra

June, 2017, 95 Pages

Abstract

A hydrothermal performance of helical annular turbulent flow in a shell and tube heat exchanger has been investigated numerically. The numerical investigation involves a three dimension numerical solution of four models by a commercial package ANSYS FLUENT 16.0. The boundary conditions of all models that solved by the numerical solution was taken as a constant temperature and constant heat flux for inner tube wall, while the outer wall of shell side was insolation. The first model has a straight annular with air flow in annular regime, while the second model has a straight annular with water flow in annular regime. The third model has a twist annular with air flow in annular regime, while the fourth model has a twist annular with water flow in annular regime. Different Reynolds number for the air and water flow inside the annular regime of heat exchanger namely (500, 1000, 1500, 2000, 2500, 3000, 3500, 4000, 4500, 5000, 5500, and 6000) were used for each model. The results indicated that the annular shape has significant effects on the hydrothermal performance; it found enchainment in all results of twist annular compared with the results of the straight annular, which included increasing in temperature difference of 9.1% and 24.2%, outlet temperature of 3.2% and 5.8%, while the increasing in heat flux, Nuselts number, and heat transfer coefficient of 11.2% and 31.3%, finally the increasing in pressure drop of 29% and 29.2% for air and water flow respectively. The results obtained from numerical solution presented the static temperature contours and showed that the temperature distribution of twist annular is better than straight annular. The present numerical results have been compared with the available previous studied and give a good agreement.

Key words: straight, twist, annular, heat exchanger, turbulent flow, performance.

Özet
SICAKLIK EŞANJÖRÜ SARMAL YILLIK TÜRBÜLANSLI AKIMININ HİDROTERMAL PERFORMANSI ÜZERİNE NÜMERİK ARAŞTIRMASI

Yüksek Lisans Tezi, Makine Mühendisliği Anabilim Dalı

Tez Danışmanı: Yrd. Doç. Dr. Munir El-Farra

2017, 95 sayfa

Özet

Bir kabuk ve tüp sıcaklık eşanjörünün sarmal yıllık akışı hidrotermal performansı nümerik olarak araştırılmıştır.Nümerik araştırma; ticari bir paket programı olan ANSYS FLUENT 16.0 tarafından geliştirilen dört modelin üç boyutlu nümerik çözümünü kapsamaktadır.Nümerik çözümleme ile çözülen tüm modellerin sınır şartları süreklik bir sıcaklık ve iç tüp duvarın ısı akışı olarak alınırken kabuk tarafının dış duvarı güneşe maruz bırakılmıştır.İlk modelin yıllık rejim üzerinde düzenli yıllık hava akımı varken,ikinci modelin yıllık rejimde yıllık düzenli su akımı bulunmaktadır.Üçüncü modelin yıllık rejim üzerinde yıllık eğri bir hava akımı varken dördüncü modelin yıllık rejim üzerinde yıllık eğri su akımı mevcuttur.Sıcaklık eşanjörü yıllık rejimindeki hava ve su akımının her bir model için kullanılan farklı Reynolds sayıları şu şekildedir(500, 1000, 1500, 2000, 2500, 3000, 3500, 4000, 4500, 5000, 5500, ve 6000)Sonuçlar yıllık şeklin hidrotermal performans üzerinde önemli etkilerinin olduğunu göstermiştir; yıllık düzenli rejimle karşılaştırıldığında yıllık eğri rejimin tüm sonuçlarında zincir bulunmuştur.Sıcaklık farklılığında 9.1% ve 24.2% oranında artış,çıkış sıcaklığında 3.2 % ve 5.8 oranında artış gözlenirken,ısı akışında,nusselt sayısında ve sıcaklık transfer katsayısında 11.2% ve 31.3% oranında artış belirlenirken sonuç olarak hava akımı basınç düşmesi ve su akımı basınç düşmesi sırasıyla 29% ve 29.2% oranındadır.Nümerik çözümden elde edilen sonuçlar statik sıcaklık kontorlarını ortaya koymuş, yıllık eğri rejim sıcaklık dağılımının yıllık düzenli rejimden daha iyi olduğunu göstermiştir.Şuanki nümerik sonuçlar mevcut önceki çalışmalarla karşılaştırılmış,iyi bir uyum ortaya koymuştur.

Anahtar kelimeler: düzenli,eğri,yıllık,sıcaklık eşanjörü,türbülanslı akım,performans

List of symbols

Symbol	Definition	Units
C_p	Specific heat	J/kg.k
I_{tur}	Turbulence intensity	
k	Thermal conductivity, turbulent kinematic \energy per unit mass	W/m.k,m^2/s^2
P	Pressure	N/m^2(Pa)
Re	Reynolds number$= \rho\, V\, d/\mu$	
T	Temperature	k
t	Time	S
U	Velocity vector	
V	Velocity	m/s
v_r	Vertical velocity	m/s
v_z	Axial velocity	m/s
v_θ	Azimuth velocity	m/s
Cµ	Coefficient to calculate the turbulence viscosity	
k	Turbulent kinetic energy	m^2/s^2
r	Cross section radius	m
$C_{\varepsilon}1$, $C_{\varepsilon}2$	Coefficient in the turbulent kinetic energy dissipation equation	
P_k, P_ε	Buoyancy forces	

Greek symbols

ι	Viscosity ratio	
ε	Effectiveness, Emissivity, turbulent kinematic energy dissipation rate	
m	Dynamic viscosity	Kg/m.s
υ	Kinematic viscosity	m^2/s
ρ	Density	kg/m^3
μt	turbulent viscosity	kg/m.s
$\sigma_{k,\varepsilon}$	turbulent Prandtl number of k,ε	
$\rho u'_i u'_j$	Reynolds stresses	

Subscripts

h	Hot in annular region,
j	Tenser symbol
$r - \theta - z$	Cylindrical-polar coordinates

Chapter one

Introduction

1.1 Background

Heat exchangers can be defined as the devices which can be utilized to transfer the heat energy between two fluids that are directly connected or may flow discretely between two channels or tubes. Heat exchangers are presented a one of the mostly equipments that are used for industrial processes and also used for transferring heat energy between two streams of process. Heat exchangers can be used in any process that includes heating, boiling, evaporation, cooling or condensation. In general, before the beginning of the process or under go to the phase change, process fluids are heated or cooled. According to the type of application, different heat exchangers are nominated. Therefore, the heat exchangers that are normally used for condensing are recognized as condensers, likewise the heat exchangers which are normally used for boiling aim are named boilers. The heat exchangers effectiveness and performance are deliberated by the heat transferred quantity by means of minimum area of the heat transferred and the pressure drop. The superior performance of its effectiveness is completed by computing the overall measurement of the heat transferred. The area that is necessary for a convinced heat transfer quantity and pressure drop offers a knowledge about requirements of power operating cost and the capital cost of the heat exchanger. A good heat exchanger design is obtained when the area is as least as possible area and pressure drop is minimum to achieve the requirements of heat transfer [1]. In the other words heat exchanger is a device which is used in order to transfer the thermal energy (enthalpy) between solid surface and a fluid, between a more fluids and between solid particulates and a fluid that at different temperatures and in the thermal contact, generally without interactions of external heat and work. The fluids may take different shapes where it is possible to be a single compound or mixture. Characteristic applications include concern fluid stream heating or cooling, multi compounds or single fluid stream processes of condensation or evaporation and heat rejection or heat loss from the system. In more applications, the objective can be for sterilize, concentrate, distill, fractionate, crystallize, pasteurize and regulator fluids of process.

In many heat exchangers, the working fluids which exchange the heat are in the direct contact. However, in the other heat exchangers, the heat transfer between working fluids take place throughout the wall of separation. Moreover, out and into of the wall in a passing means. In the most heat exchangers, the working fluids can be separated by the surface of heat transfer, and preferably they do not mix. These exchangers are mentioned to the direct transfer kind or the simply recuperates. Alternatively, the exchangers with an intermittent heat exchange between the cold and hot fluids through thermal storage of energy and rejection through the exchanger surface or the matrix are called as the storage type, indirect transfer type or simply regenerators. [2].

1.2 Heat Exchanger Classification

There are many configurations which through the heat exchangers can be obtained. The heat exchangers can be divided depending on their application, process of fluid flow and mode of heat transfer as follows [3]:

1.2.1 According to the heat transfer process

They include the following types:

- Direct contact type Heat exchangers are known as the heat exchanger where the two operating fluids are mixed directly with each other in order to transfer the heat between two operating fluids. This type of exchangers gives high efficiency compared with another types of heat exchangers.

- Recuperate type or Transfer type heat exchanger where the two fluids are concurrently flow throughout two tubes which are detached by the walls.

- Regenerator type heat exchanger where the cold and hot fluid flow in alternative form on the same surface. Through the transference of the hot fluid, the exchanger wall get heated and when the cold fluid flows through it, this heat will be transferred from the wall of the heat exchanger to the cold fluid. Therefore, the cold fluid temperature will be increased. Blast furnace and pre-heaters for steam power plant are the communal examples of this type of heat exchangers.

1.2.2 According to the Constructional Features

They include the following types:

- Tubular heat exchangers are positioned concentric with together and two operating fluids flow in two tubes which are detached by a wall. In general, they can be used in most of the engineering applications.

- Heat exchanger of tube and shell type which involve of shell and single or great parallel tubes number. The heat transfer with take places when one of fluid flows inside the tube and another flows outside of the tube inside the shell of the exchanger. The surface area to volume of this type of heat exchanger is so large. Baffles plates are delivered in order to improve the turbulence and therefore, the ratio of heat transfer.

- In order to enhance the ratio of heat transfer, fins are delivered on the external surface of the heat exchanger. They are used in generally in type of gas to liquid heat exchanger and fins are usually delivered in gas side. Also, they are used in heat pumps, gas turbines airplanes, automobiles and in other applications.

1.2.3 According to the flow arrangement

They include the following types:

- Type of parallel flow heat exchanger in which two working fluids flow parallel together and thus, they are flowing in the same direction. As well as, they are named as concurrent heat exchanger.

- Counter flow heat exchanger in which two fluids flow in an opposed direction.

- Cross flow type heat exchanger in which two fluids flow vertical to each other. This is additional separated in to mixed and unmixed flow type heat exchanger [4].

1.3 Applications of Heat exchangers

In order to describe the heat exchangers applications, a comprehensive investigation must be implemented to cover all of their features because they are huge and varied applications in different fields. However, there are communal application of the heat exchangers including in the home applications, mechanical

equipment industry and process industry. Currently, heat exchangers are used generally in heating district systems. As well as, heat exchangers are set up in air conditioners and refrigerators in order to condense or evaporate the working fluid. Furthermore, they are used in treatment of milk for the sake of pasteurization. Table 1 explains the application of heat exchangers in details in different industries [5].

Other applications of heat exchangers are include process plants, nuclear plants, power generation plants, food processing industries, heat recovery systems and in cryogenic applications [4].

Table 1.1 Heat Exchanger Applications in Different Industries [5].

Industries	Applications
Food and Beverages	Milk Pasteurization, ovens, cooling Food processing and pre-heating, juices and syrup pasteurization, cookers, beer cooling and pasteurization, or chilling the final product to favorite temperatures.
Petroleum	Fluid interchanger cooling, Brine cooling, acid gas condenser, crude oil heat treatment and crude oil pre-heating.
Hydro carbon processing	Recovery or removal of carbon dioxide, ammonia production, Preheating of methanol, liquid hydrocarbon product cooling and feed pre-heaters.
Polymer	Polypropylene production and reactor jacket cooling for polyvinyl chloride production.
Pharmaceutical	Water and steam purification and use cooling for point on Water For Injection ring.
Automotive	Painting, Pickling, Priming and Rinsing.
Power	Oil coolers, energy recovery, cooling circuit, air conditioners and heaters Radiators.
Marine	Cooling of lubrication oil Systems of Marine cooling, Diesel fuel pre-heating, Central cooling and Fresh water distiller.

In this study, we will investigate shell and tube heat exchanger.

1.4 Shell and tube heat exchanger

The shell and tube heat exchangers are the most communal types of heat exchangers which are used in the industrial applications as shown in Figure (1.1). There are a great number of tubes for shell and tube heat exchangers that may reach to several hundred packed in the shell throughout their parallel axes of the shell. When one working fluid flows outside tubes in the shell regime and another one flows inside the tubes regime, the heat transfer occurs. Normally, baffles are placing in the shell regime to make force in the shell side working fluid to flow stream through the shell for enhancement heat transfer and preserve identical space among the tubes. In spite of the extensive applications for shell and tube heat exchangers, they are not appropriate to be used in the automotive and aircraft because of their big size and weight. The tubes that existed in shell and tube heat exchanger are opened to the large flow areas that named as headers in all of the shell ends of a shell where the tubes side working fluid accumulated before the tubes entered the tubes and after the tubes leaved them. Moreover, shell and tube heat exchangers are additional categorized rendering to a number of the shell and tube permits complicated Heat transfer balance for shell and single tube is shown in figure (1.2) [6].
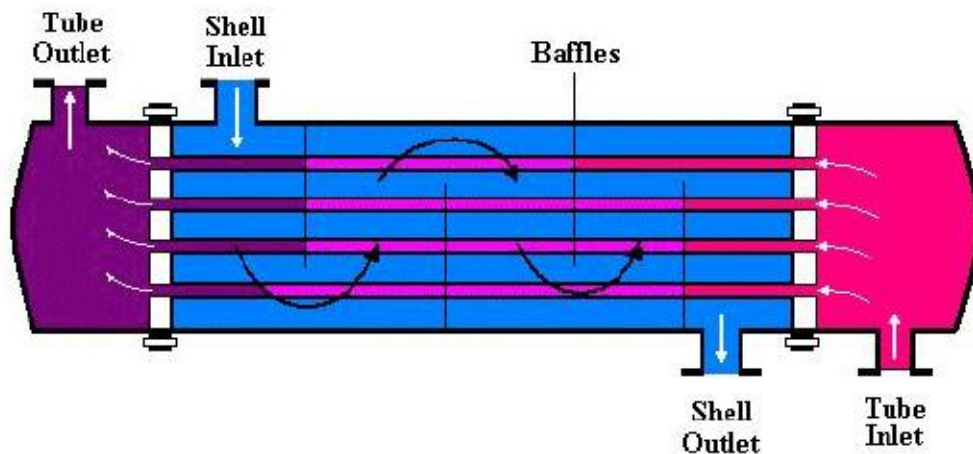
Figure 1.1 Shell and tube Counter-current Heat Exchanger Arrangement [6].
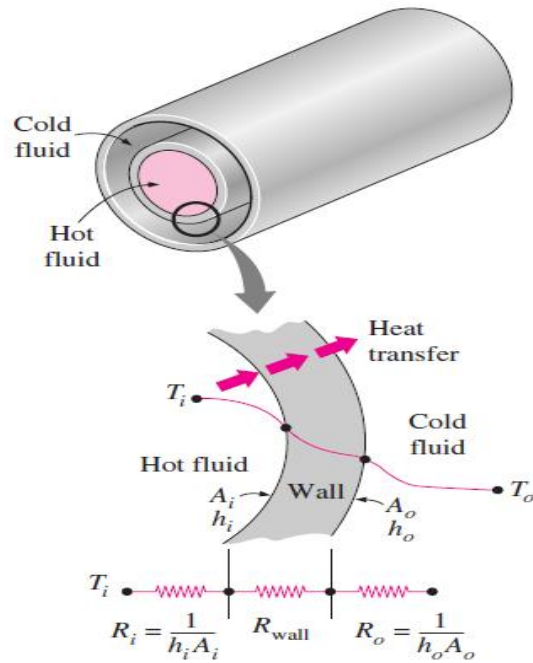
Figure 1.2 Heat transfer balance for shell and single tube [6].

1.5 Objective of work

The main aims of this investigation are:

1- Numerically study the effect of the helical annular turbulent flow on the hydrothermal performance of shell and tube heat exchanger.

2- A comparison of the hydrothermal performance between straight and helical annular shell flow.

Chapter Two

Literature Review

2.1 Introduction

Annular flow geometries continue to be important in many engineering applications. These include fuel assemblies, propulsion systems and heat exchangers in atomic reactors. Many of these devices operate under conditions in which property variations are expected to influence greatly the velocity and temperature distributions. Many requirements have been dictated in order to develop the components of the nuclear fuel. Practically, in most of the cases, the specifications of different reactor require that the fuel assemblies designed to suit each case separately. At this process, there is an important point that must be taken into consideration which is the generated heat in the fuel must be transferred effectively to the coolant. The coolant channel takes a basic form which is annular passage. Therefore, it is essential to analyze the turbulent flow features in the annular passage to realize the problems of heat transfer implicated in the design of nuclear fuel element. Since coiled tube-in-tube heat exchangers deliver a big surface area per unit volume, they are extensively used in HVAC applications. The process of designing these exchangers needs a knowledge of heat transfer measurements for coiled annular ducts and coiled circular tubes. Correlations for predicting heat transfer in coiled circular tubes are available in the literature; however, few works has been reported on coiled annular ducts.

CFD modeling is used in the prediction of turbulent flows with comparison with experimental data for annular flows under variable property conditions. Difficulties associated with accurately modeling the turbulent flows. Types of researches that interested in annular turbulent flow are:

1- Plain annular flow researches.

2-Researchers used rotating tube or shell to simulate helical or swirl annular flow.

3-Researchers studied the effect of inserted helical soled wire or twisted tape in the annular region on hydrothermal performance of flow.

2.2 Plain annular flow researches.

Barletta and Lazzari, (2005) [7], studied theoretically under the hypotheses of parallel and fully developed flow the laminar mixed convection of a Newtonian fluid in a vertical annular duct subjected to no axisymmetric thermal boundary conditions as shown in figure 2.1. The Boussinesq approximation has been employed and the viscous dissipation impact has been deliberated as insignificant. Fourier series approach has been used to solve the equations of momentum and energy balance. Furthermore, the element of Fanning friction and the dimensionless pressure drop parameter have been specified. The field of dimensionless temperature while the dimensionless velocity distribution, the factor of fanning friction or the dimensionless pressure drop factor are influenced by the buoyancy effect. The downward flow and upward flow of the threshold values have been evaluated analytically. The general solution has been applied for many of cases such that one wall is kept isothermal and the other wall is half adiabatic and half exposed to a uniform inward heat flux distributions. Particularly, the second example refers to an annular duct with an internal isothermal wall and an external wall half adiabatic and half heated with a uniform heat flux.
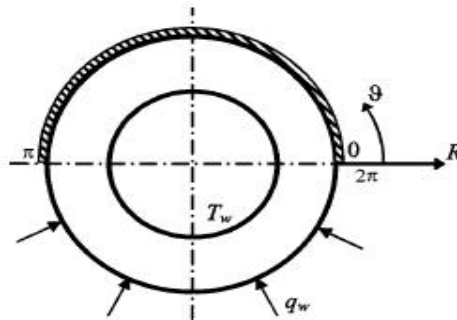
Figure 2.1 Section of the annular duct with prescribed thermal boundary conditions [7].

Khalil et al., (2008) [8], studied analytically and numerically the laminar flow demeanor in concentric annulus with moving pulp in pipe as shown in figure 2.2. The analytical analysis was given as exact solution for steady one dimensional fully developed flow. The numerical model has been introduced to axisymmetric, steady two-dimensional model, evolving and completely advanced flows. A staggered grid was used for numerical model with using pressure adjustment method. The analyses have been used in order to forecast the profile of developing velocity and fully developed velocity, zero, and gradient of adverse pressure. At different Reynolds numbers the thickness of the boundary layer, entrance length, and the spreading of pressure alongside the moving core were obtained via presented model. For laminar fully developed flow, numerical solutions were agreed with the analytical exact solution.
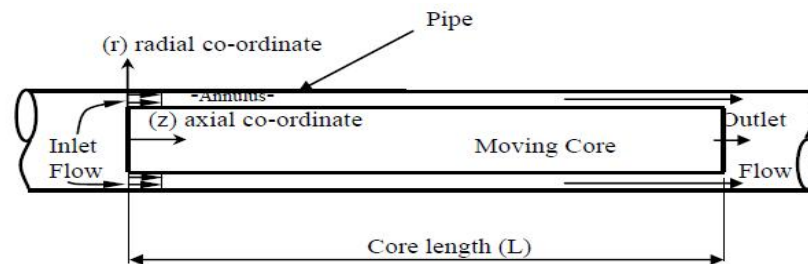
Figure 2.2 Schematic lustration for long concentric moving core in pipe[8].

Han et al., (2009) [9], investigated experimentally the vertical upward hydraulic transport of solid-liquid mixture of solid elements by non-Newtonian fluids in narrow concentric annulus with rotating inside cylinder. The particles of solid movement have been detected by clear acrylic pipe. Annular speed ranging from 0.4 to 1.2 m/s. Pressure drops and solid volumetric concentration were measured for various flow rate, inclination angle, and rotational speed of inner cylinder.

Boersma and Breugem, (2011) [10], calculated the fully developed turbulent flow in concentric slim annuli by using direct numerical simulation. The outer tube diameter is greater than 10% of the inner tube diameter. The surface area of inner tube was smaller than the outer pipe surface area. The extra stress on the flow that

generated from inner annulus small surface area was negligible. The flow patterns in the inner annulus was different from floe pipe pattern and scaling properties was raised. The velocity profile near the inner annulus was logarithmic. In direct numerical simulation observed that there was no shift among the point of zero shear stress and the ultimate axial velocity which was contrary to what had been mentioned in the literatures.

Hong et al., (2011) [11], investigated numerically gaseous flows heat transfer characteristics in concentric tubes of micro annular with heat flux which can be positive or negative constant. The micro annular tubes of energy equations and compressible momentum with slip boundary conditions have been answered. Arbitrary Lagrangian Eulerian method was the bases of numerical methodology. The calculations have been implemented for two thermal cases; (a) the continuous heat flow which at the internal wall whereas external wall was adiabatic, and (b) the continuous heat flux at the external wall whereas the internal wall was adiabatic. The radius of the external tube vary between 20 µm to 150 µm with radius rates of 0.02, 0.05, 0.1, 0.25, and 0.5 and one hundred was the length rate to hydraulic diameter. The outlet pressure is fixed at the ambient pressure of atmospheric. Figure 2.3 explains the temperatures of bulk and wall with positive and negative heat flux that have been compared. The compressible Nusselt number slip flux is varied from that of incompressible flow. A correlation was proposed for prediction the properties of heat transfer of gas slip flow through the concentric micro annular tubes.
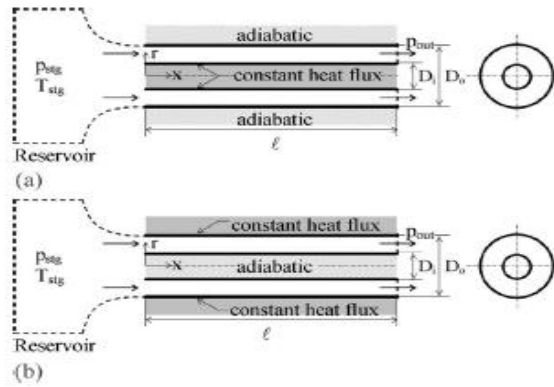
Figure 2.3 Schematic diagram and boundary conditions [11].

Shaker, (2012) [12], studied numerically the development of laminar flow through the entry and troubled areas of annular circular pipes as was shown in figure 2.4. Both main and disturbed pipes were stationary and concentric. The non-uniform developing flows arises at the concerned areas of annular concentric disturbed pipe whereas, the uniform developing flow arises in the main pipe entrance area and at the disturbed area of the inside disturbed pipe. Numerical solutions are obtained for two-dimensional problem for Reynolds number 25 to 375. The pressure drop and velocity within the complete channel have been computed by auto FEA software. The extreme velocity at the pipe centerline and hydrodynamic boundary layer have been developed quicker for the lesser Reynolds number. Nevertheless, at the entire studies, the flow field was same. The whole date of the current studies were in moral agreement with Auto FEA software. In the centerline of the disturbed pipe, the axial velocity is increasing until reach to the greatest point. The velocity outline in the annulus concentric unit of troubled pipe is non-uniformly spread. Since the velocity impact at the inlet annulus unit, the velocity that is close to the disturbed pipe is greater than the velocity that is close to the main pipe. The flow ratio decrease close the walls that because of the friction should be recompensed by a consistent increase close the axis because ratio of the volume flow is constant. In the entry area the greatest velocity decreased with increasing Reynolds number but the velocity close the wall increased with increasing Reynolds number. The outlines of velocity in completely developed was Reynolds number independent. The dimensionless pressure in the inlet unit is one and increase with decreasing space in Z-direction because of the friction. The dimensionless pressure increased quicker with the

11

increasing of Reynolds number. The drop of pressure in the inside area is less than the drop of pressure in annulus area.
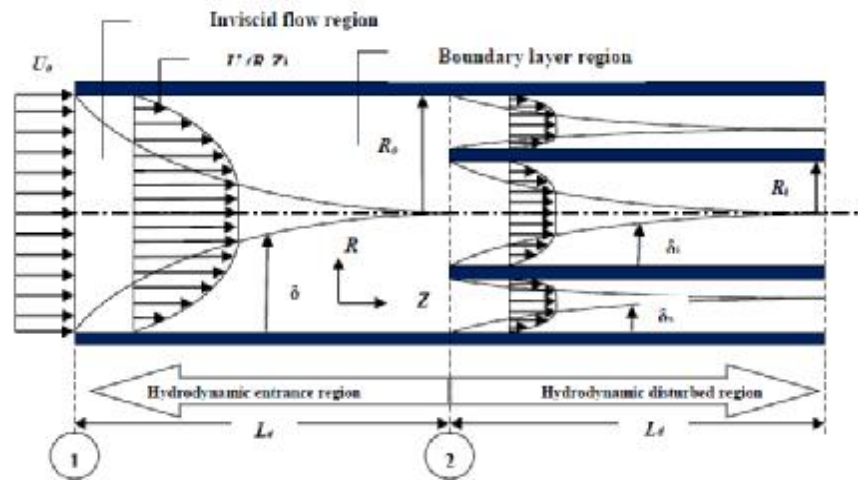
Figure 2.4 laminar, hydrodynamic boundary layer development in a concentric circular pipe [12].

Nebuloni and Thome, (2012) [13], investigated numerically the model of concerning annular film condensation in micro channels of various inner shapes comprising nonuniform heat flux and wall conduction impact to answer the problem of conjugate heat transfer. The three wall boundary conditions of external channel was: a non-uniform wall heat flux, temperature of a uniform wall, and existing a cooling single phase convective. Through the move from the mini channel to micro channel, the scale was reduced and the axial conduction become important in profile of founding wall temperature and heat transfer factor along the channel. It is found that the annular condensation heat transfer factor is heavily depend on the geometrical shape of the internal channel, characteristics of wall thermal, and the heat flux spreading. It can be said at small percentage the capillary forces can improve the total thermal performance expressively. The entire performance that relies on high coupling between the inner and outer heat transfer with the channel conduction properties has been recognized. For annular laminar film summarizing, the factor of the heat transfer is improved when the supply of heat transfer nonuniform. Despite that this causes strong spatial oscillations for the temperature of the channel wall.

Maudou et al., (2013) [14], studied experimentally the upward flow of convective hate transfer in vertical , open-ended annular channels with a diameter ratio of 0.61, an aspect ratio of 18:1. Also, at the same study they used both inner surfaces heated consistently with mixed convection system and some overlay with the forced convection system explained in figure 2.5. The eccentricities varieties were from 0 (concentric annulus) to 0.9 (near contact) and three inlet bulk Reynolds numbers which is almost equal to 1500, 2800, and 5700. The small eccentricity was up to nearly 0.3 and had insignificant impact on the entire ratio of the heat transfer. Nevertheless, more increasing eccentricity resulted in an important heat transfer decrease. The ratio of average heat transfer for eccentricities higher than 0.7 was lower up to 60% of that at concentric circumstances. The temperature of the wall in the open channel area was much lower than the temperature in the narrow gap area. The average Nusselt number increased weakly at faster ratio for concentric annuli, with increasing Reynolds number up to 2800. The Dittus–Boelter correlation was lower the concentric-case Nusselt number while the highly eccentric-case Nusselt number was expressively lesser than that.
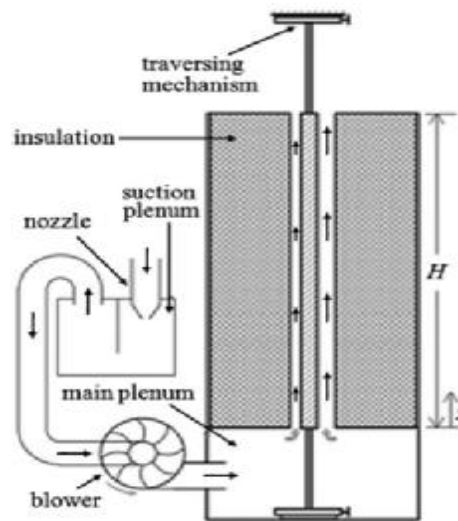
Figure 2.5 Schematic diagram of the experimental apparatus [14].

Yang et al., (2013) [15], studied experimentally the supercritical water heat transfer in a vertical annular tube, 2 mm annular gap and an inner heater of 8mm outside diameter, downward and upward flow at test pressures of 23 and 25 MPa, mass fluxes of 700 and 1000 kg/m².s, and heat fluxes of 200–1000 kW/m² of Heat-transfer properties were differences between the directions of two flow. The element

heat transfer of increasing flow was greater than downward flow. Spacer at downstream of the annuli, was effected strongly on heat transfer regardless of flow direction.

Aly, (2014) [16], investigated numerically the flow of 3D turbulent and heat transfer of twisted tube-in-tube heat exchangers as shown in figure 2.6. The heat transfer and turbulent flow in the heat exchanger have been simulated by using the realizable k-e model with improved wall treatment. The twist diameter ranging from 0.18 to 0.3 m while the flow ratios of tube and annulus from 2 to 4 and 10 to 20 LPM respectively. At this investigation, it has been used the temperature reliant thermos physical characteristics of water. Conjugate evaluating of heat transfer was used from hot fluid in the inner-coiled tube in order to cold fluid in the annulus region. The supreme significant design factors in coiled tube-in-tube heat exchangers are annulus side flow rate, tube side flow rate, coil diameter, and flow configuration, respectively.
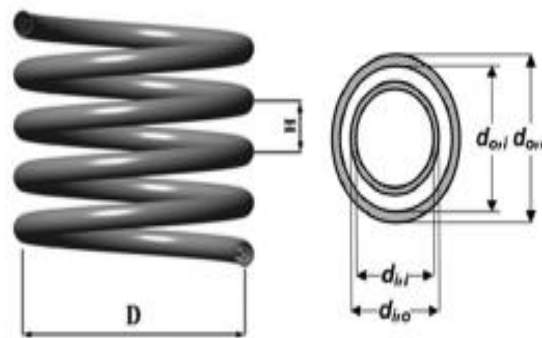
Figure 2.6 Schematic diagram and coordinate system of the tube-in-tube heat exchanger [16].

Kanaris et al., (2015) [17], performed direct numerical simulations of the three-dimensional turbulent flow in an annular duct of unit eccentricity as shown in figure 2.7. Three diameter ratios have been investigated, namely a = 0 (plain circular pipe), a = 0.1395 and a = 0.2591, while the Reynolds number was kept constant at Re = 14600. The diameter ratio impact on the drop of pressure and friction factor has been shown. Also, clarify the effects of secondary mean motion, at small diameter ratios, on the flow characteristics and vortex structures.

Schematic represantation of flow configuration.
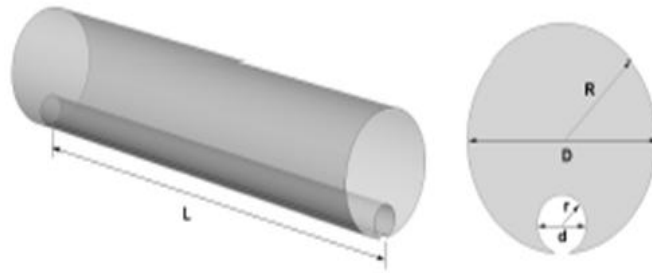
Figure 2.7 Schematic representation of flow configuration [17].

Kline and Tavoularis, (2016) [18], studied experimentally as shown in figure 2.8 the effect of eccentricity varying from 0 to 0.9 on forced convective heat transfer for upward flows with Reynolds numbers Re=5450, 10,000 and 27,500 in open-ended annular vertical channels the rate of diameter ratio is 0.61. The distance to external rate of diameter is 18:1 and inner surfaces were heated consistently. The eccentricity effect was not important at the minor peculiarities. Through the extremely eccentric cases, the temperature of the wide annulus was lower than the temperature in the narrow annulus. For Re>10,000, the average Nusselt number for the concentric case was approximately four times greater than the value that have been expected by the correlation of Dittus–Boelter. Through the comparison with the concentric case, the inclusive heat transfer factor in greatly and temperately eccentric annuli was concentrated by up to 80%. Major eccentricity presented great azimuthal differences in the temperature of the local wall (the temperatures of higher wall witnessed in the narrow gap) and heat transfer factor. For the whole eccentricities, the average Nusselt number enlarged monotonically with growing the Reynolds number.
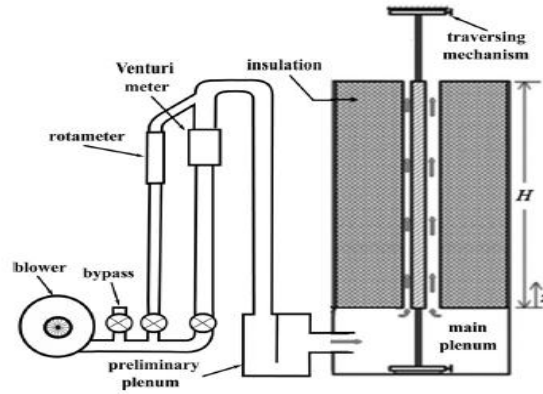
Figure 2.8 Diagram of the experimental apparatus [18].

Aly, (2016) [19], numerically studied the heat transfer behaviors and laminar flow of nanofluids (CuO/water, Al2O3/water) flowing by the annular coiled tube as shown in figure 2.9 with constant wall temperature boundary. The replications which enclosed a nanoparticles volume concentrations of 1.0–6.0% and mass flow ratios from 0.025 to 0.125 kg/s. The practical results pointed that the nanofluids has enhanced the heat transfer. The factor of heat transfer and pressure drop with the same Reynolds number have increased with the concentration increase of a particle volumetric. The extreme heat transfer factor developments were 44.8% and 18.9% for CuO/water and Al2O3/water, respectively. The loss of pressure was around seven times for CuO/water nanofluid in association to water and seven times for CuO/water nanofluid. Moreover, in comparison to water, nanofluids at concentrations up to 3% delivered the same heat transfer quantity at minor propelling power.
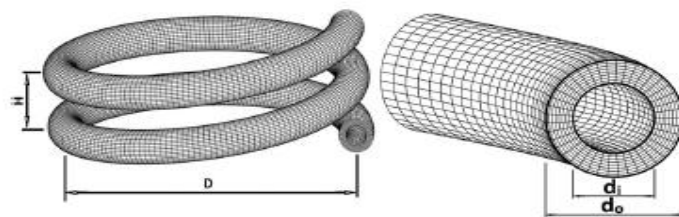
Figure 2.9 Geometrical parameters and grid system of the annular coiled tube[19].

2.3 Researches used rotating tube or shell to simulate helical or swirl annular flow.

Lee et al., (2005) [20], investigated numerically the flowing of air upward in a vertical annular pipe with a rotating outside wall as shown in figure 2.10. The goal of this simulation was the variations of linearization and property for high heat flux heat

16

transfer. The equations compressible filtered Navier- Stokes have been solved by using the second-order precise finite volume approach. Turbulent kinetic energy decrease has been recognized and the intensity of bursting decreased close the wall of nonrotating. Stream wise velocity spreading variance because of the effect of rotating outer wall. The axial velocity profiles near the rotating wall approached a laminar profile, while turbulent velocity profiles were preserved close the nonrotating wall. Since the turbulence enhanced near the stationary heated inner wall, the Nusselt number was increased.
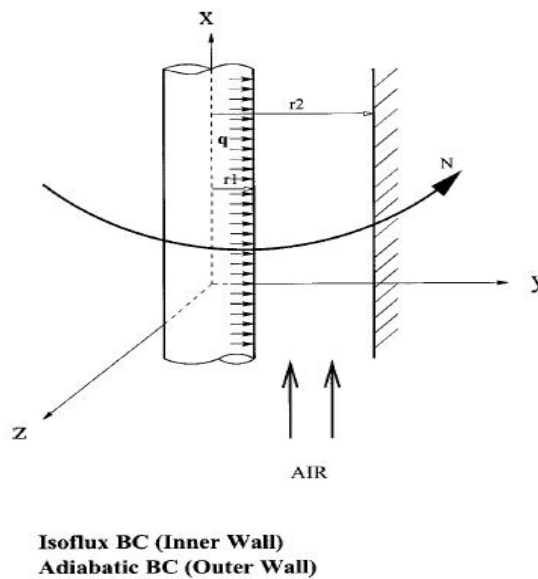
Figure 2.10 The configuration for annular pipe flow with outer wall rotation[20].

José et al., (2008) [21], solved numerically convection-diffusion equation of 3D laminar flow in the eccentric helical annular heat exchanger where the external cylinder turns at a continuous velocity. Whereas the internal cylinder rotated in opposite direction, as shown in figure 2.11. Rotation cylinders produced chaotic advection in the eccentric, which that enhanced the thermal efficiency. When both cylinders turn at constant velocity, largest thermal efficiency was obtained with highly eccentric configurations. Highly thermal efficiency obtained with high frequency range was more than obtained for steady boundary rotation where chaotic advection can be stimulated efficiently.

17
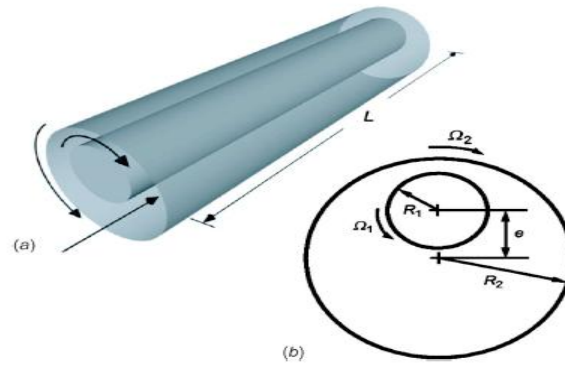
Figure 2.11 Sketch of (a) Eccentric helical annular heat exchanger and (b) its cross-sectional geometry[21].

Abou-Ziyan, (2016) [22], studied through the practical experiment the heat transfer and pressure drop in concentric annular wide channel with internal finned pipe or plain through the rotating and stationary conditions as shown in figure 2.12. The experiments were conducted for three finned pipes and one plain pipe with helical fin space of 75, 110 and 150 mm at rotating speeds of 0, 200, 250, 300, 350 and 400 rpm. The experiments has been covered the axial Reynolds number of 80700, 182000, and rotational Reynolds number of 0 and 1428 to 3008, relates to Taylor number of 0 and from 1.22*10^6 to 8.32*10^6. Nusselt numbers and friction factors were associated in terms of Ta, Re, Pr and fin geometrical factors. At Re = 1.5*10^5, annular channel with internal pipe of helical fin space 75 mm that rotates at 400 rpm enhanced Nu by a factor of 7.5 and pumping power increased by a element of 7.6, associated to simple standing pipe.
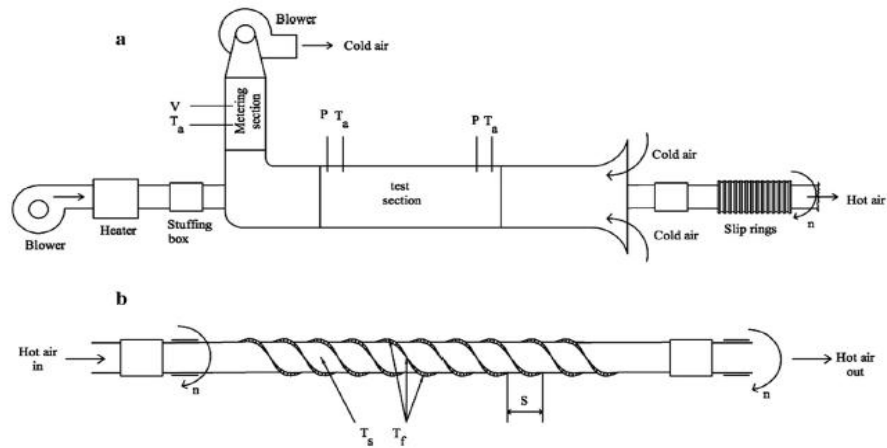
Figure 2.12 A Schematic diagram of the experimental apparatus, (a) Layout of the experimental apparatus, (b) Details of the inner rotating pipe showing the interrupted helical fins[22].

2.4 Researchers studied the effect of inserted helical soled wire or twisted tape in the annular region on hydrothermal performance of flow.

Garimella et al., (1988) [23], explored through the practical experiment the heat transfer of forced convection in coiled annular pipes and have been observed a combination of the curvature effects, the wire insert and the annular cross section as shown in figure 2.13. At this study, there are two annulus radius ratios and two coiling diameters have been used. Laminar and transition flows average heat transfer coefficients were obtained where Augmentation in the laminar flow was higher than in the transition regime. The heat transfer coefficients of annulus coiling were beyond the values for a conventional annulus specifically in the laminar area and the augmentation reductions where the flow arrives the transition area. The concentric annulus with curvature and a twisted wire insert leads to heat transfer augmentation. Transition set in around a Dean number = Re*((do-di)/D)^0.5 of 300-375. Dean number was one of the governing factors for laminar flow heat transfer and the importance of the coiling ratio (do-di)/D decreases in the transition region.

19
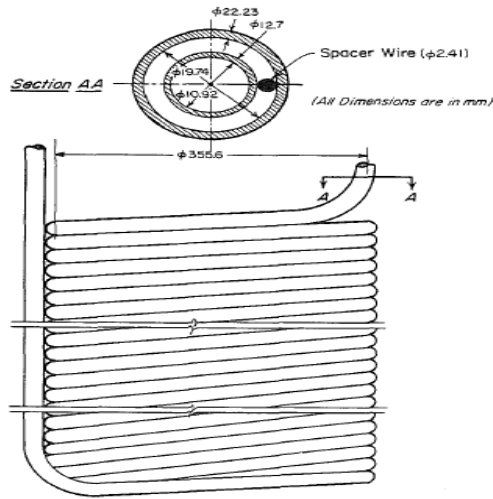
Figure 2.13 Schematic of coil tube[23].

Gupte and Date, (1989) [24], measured experimentally friction and Nusselt number data for helical flow in annuli that was generated via twisted tape as shown in figure 2.14, for radius rates of 0.41 and 0.61 and twist ratios of ∞, 5.302, 5.038, and 2.659. At the same Reynolds number depending on the hydraulic diameter, the increases in drop of pressure and heat transfer factor over an empty annulus were 90% and 60%, respectively. Excellent analytical predictions depending on the analogy that existed between heat and momentum transfer and on principle of superposition of pressure drops for twist ratios ∞ and 5.302 were found. The measurements of pressure drop and heat transfer had agreed 15% with the well-accepted correlations for noncircular ducts.
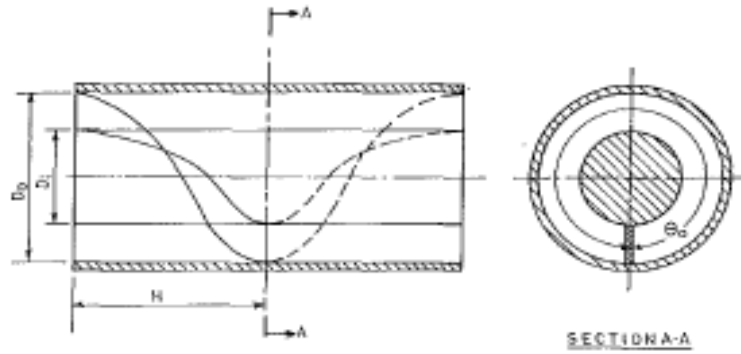
Figure 2.14 Geometry of an annulus with helical tape[24].

Jawarneh ,(2007) [25], was simulated turbulent flow in a narrow concentric annulus as shown in figure 2.15 and investigated forced convective heat transfer and the characteristics of decaying swirling flows. Approach of finite volume was used to answer numerically the prevailing equivalences. Adiabatic wall at the external wall and the temperature of uniform wall in the internal wall were considered as thermal boundary conditions. Nusselt number and the axial and swirl velocity distributions were obtained for different values of the Reynolds number and inlet swirl number. The inlet swirl number has great influence on the heat transfer characteristic. The heat transfer in developed flow region was enhanced as the inlet swirl number was increased. Centrifugal forces in the annulus lead to existence of secondary flows. The axial velocity near the wall was increased as the inlet swirl number increases while the axial velocity reduced at the mid annular to achieved the conservation of mass. Increases in velocity near the wall, lead to higher heat transfer rate and larger temperature gradient. Downstream of flow the swirl velocity profiles decay gradually due to the friction that damped the tangential velocity.
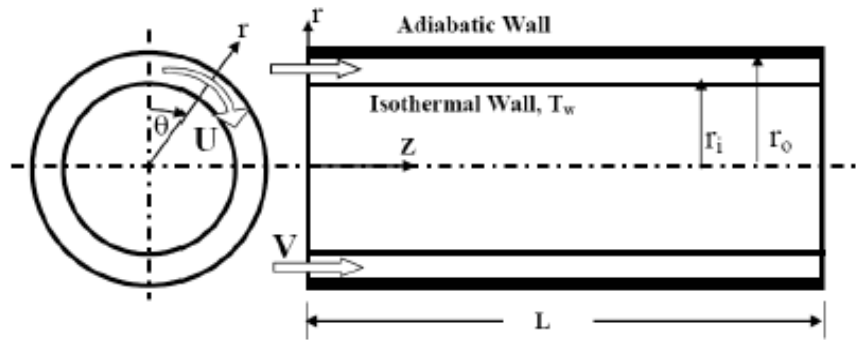
Figure 2.15 Swirling flow between concentric cylinders[25].

Poskas, et al., (2011) [26], investigated experimentally the heat transfer from the walls of convex and concave of air flow in the channels of rectangular helical as shown in figure 2.16 with two-sided heating at Re = 1000 to 200000 and comparative curvature D/h = 5–90 and comparative width b/h = 2–20. For two-sided heating Nu numbers of concave and convex walls increased until 20% in compare with one-sided heating. The average of heat transfer in the helical channels rises until 50% and 20% for laminar-vortex flow and turbulent flow in contrast with traditional flat channel heat transfer.
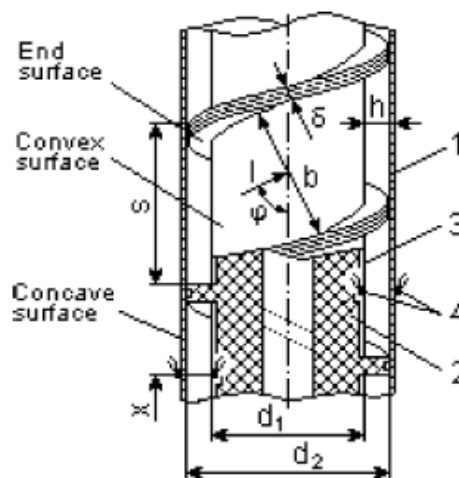
Figure 2.16 Geometry of rectangular cross section helical channel: (1) calorimetric tube; (2) textolite worm insertion; (3) calorimetric foil and (4) thermocouples[26].

Genic et al., (2012) [27], investigated experimentally the measurements of thermal performance for 3 heat exchangers with concentric helical coils as shown in figure 2.17. The consideration was paid on element of shell-side heat transfer that is intensely prejudiced by winding angle, axial pitch, radial pitch, etc. This study has

discovered the following correlation Nu = 0.50 * (Re^0.55) * (Pr^ 1/3) * ((Ɲ/Ɲw)^0.14) where Nu and Re are based on shell side hydraulic diameter. The element of shell-side heat transfer must depend on shell side hydraulic diameter due to that this factor consists shell side construction factors number.
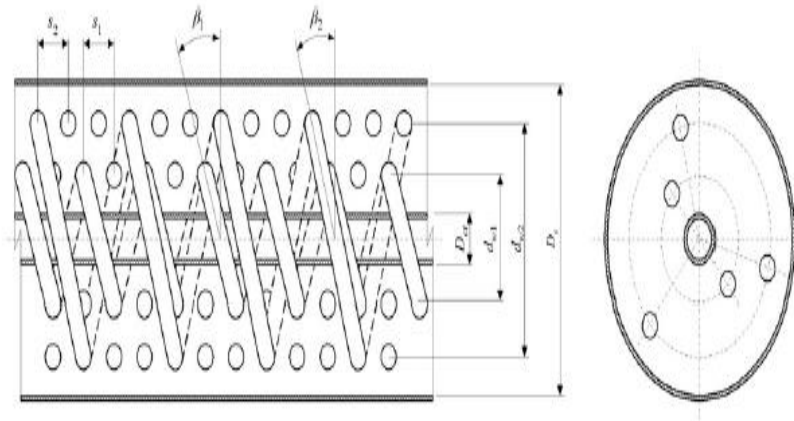
Figure 2.17 Heat exchangers with concentric helical coils[27].

Chen et al., (2015) [28], studied experimentally and numerically the flows of swirling decaying and the pipe of annular as shown in figure 2.18. A series of work has been done on studying the improvements of heat transfer by using passive approaches. As well as, the fluid dynamics of swirling decaying flows which have been created via axial vanes set in the concentric annular pipe. The simulation model has been used for the heat transfer and fluid flow of swirling decaying flows in an annular pipe. Predicted cooling curves had validated and had similar behavior with experimental cooling curves.
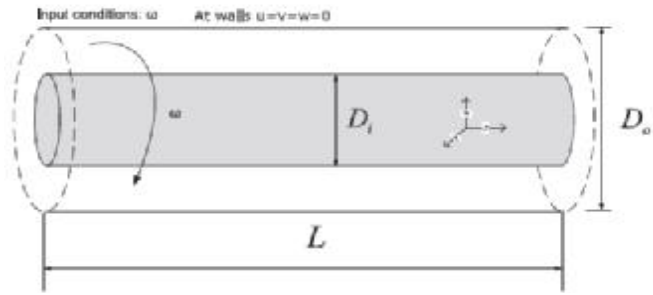
Figure (a) Physical model of a rotating pipe[28]
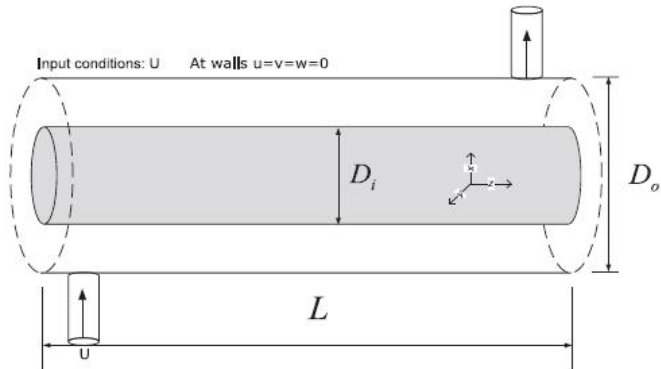
Figure (b) Physical model of a tangential inlets[28]
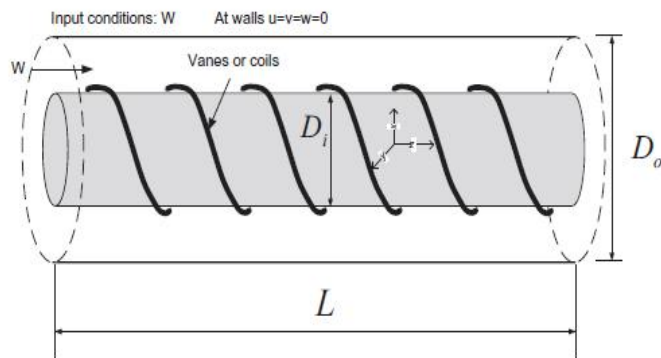
Figure (c) Physical model of guided swirls[28]
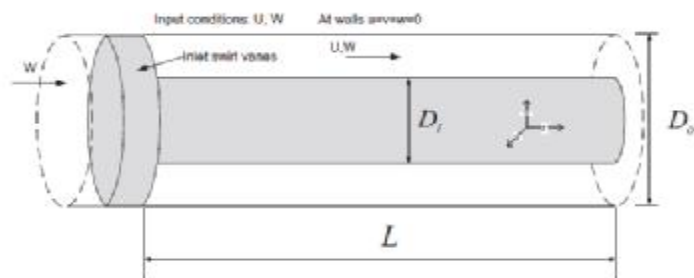
Fig. 4. Physical model of inlet axial and radial swirlers.

Figure 2.18(d) Physical model of inlet axial and radial swirls[28].

Mali et al., (2016) [29], studied experimentally the passive augmentation technique named centrally hallow twisted tape in tubular heat exchanger as shown in figure 2.19, for the improvements of heat transfer under laminar flow condition. At the persistent wall heat flux boundary condition experimentation was done with Reynolds number 600 to 1600 with step size 200. As centrally hallow width increased enhancement of heat transfer was increased and maximum enhancement was happened when hollow width of 8 mm. Increasing of nanofluid concentration lead to enhancement increased. Overall heat transfer enhancement of the centrally hollow twisted tape was increased by 22.4% as was compared to conventional twisted tape also the increased in friction factor was less as it compared to rise in heat transfer.
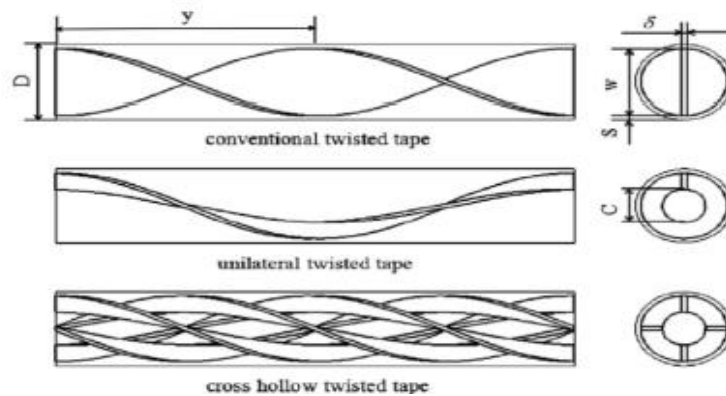
Figure 2.19 tube fitted with conventional, unilateral, and centrally hollow twisted tape[29].

2.5 Summary of Previous Researches

Review of previous works showed two types of researches that studied the effect of annular helical flow; one used inserts in the annular region in order to generate the helical swirl flow and the second used rotate inner tube or shell or both of them in order to produce helical swirl flow.

2.6 Originality

From all the literature survey that reviewed, no theoretical works are made simulation model of inserted twisted tape in the annular space and solved the turbulent helical annular flow numerically to predict the hydrothermal performance with two type of boundaries conditions:

- Constant tube wall temperature with isothermal shell surface.
- Isothermal tube wall surface with persistent heat flux on the shell surface.

2.7 Scope of the Work

In these listed points below, are summarized the scope of the work of this thesis.

1- Review all recent related work (reports, documents, researches or theses).

2- Model the problem with the suitable mathematical model and assumptions, defining the boundary conditions and auxiliary relations needed.

3- Solve the mathematical model in 2 numerically.

4- Develop a computer program to implement the discretized model in 2 and 3

5- ANSYS fluent 16 is used to solve the model case study, while the mesh is done by using Pointwise program. The case study is tube heat exchanger and Four meter shell. Tube outside diameter is 19mm while the inner shell diameter is 39 mm. The boundary condition of outer surface of tube is constant wall temperature while the shell surface is isothermal. Water and air is the fluid that will be used in the annular helical shell.

6- Represent and analyze the results for final conclusions.

Chapter Three

Theoretical Model and Numerical Solution

3.1   Numerical Solution (Computational Fluid Dynamic)

This chapter presents the mathematical models for shell and tubes heat exchanger. The present models involved the basic conservation principles of the mass, momentum, and energy. This motivates to the necessity of developing the prevailing equations for the heat transfer and fluid flow which are used to analyze the steady state conditions.

Three-dimensional, turbulent flow with compressible and incompressible flow are considered in this study to estimate the thermal performance and pressure drop for fluids flow in the straight and twist annular region of heat exchanger for different velocities of water and air in the straight and twist annular region.

ANSYS - Fluent version 16 is used to solve the models cases study, while the mesh is done by using Pointwise program. Four meter long of shell and tube heat exchanger is employed in this study. Tube outside diameter is 19mm while the inner shell diameter is 39mm. The boundary condition of outer surface of tube is constant wall temperature while the shell surface is adiabatic. Water and air is the fluid that will be used in both straight and annular helical shell for the geometry models with using a computer with Intel core I 7 processer at 1.7 GHz speed and Ram of 32 GB.

3.2   System Geometry

This present work includes models geometry of shell and tubes heat exchangers as shown figure (3.1) and the specifications of present models are shown in table (3.1).

Table 3.1 Specification of Present models

Model Name	tube section Shape	Outlet tube diameter(mm)	Shell section Shape	Shell dimensions (mm)	Height (mm)
Straight	circular	Do=19	Circular	Di =39	4000
Twist	circular	Do=19	Circular	Di =39	4000
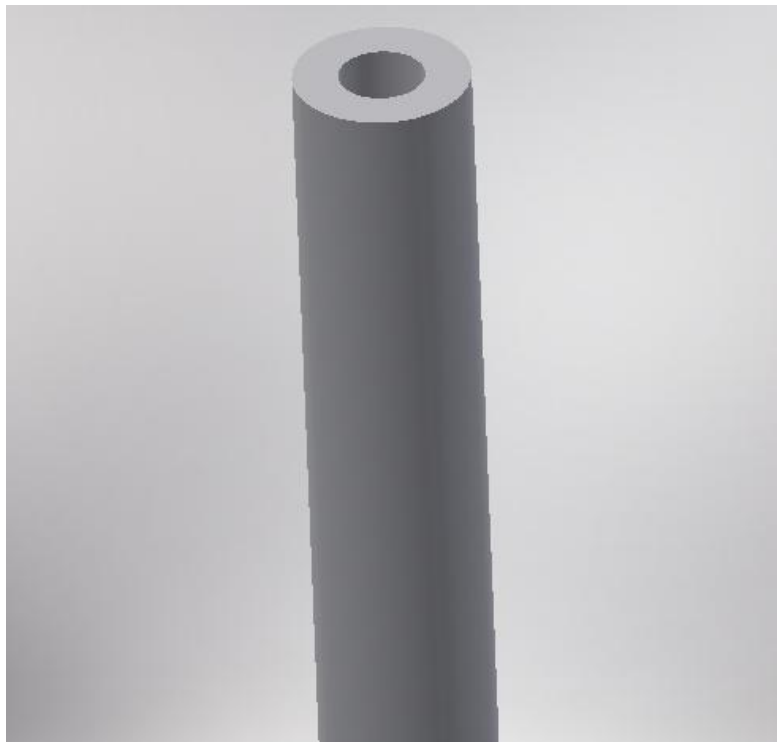
(a)

(b)

Figure 3.1 Geometries of present models: (a) straight annular model, (b) twist annular model

3.3 Assumptions

The assumptions that considered for the present investigation are:

1. The models are simulated under steady state conditions.

2. The working fluids are air (compressible) and water (incompressible).

3. Three dimensional polar coordinates model is considered.

4. No heat Source.

5. Insulation outer wall of annular regime, that means no heat flux from outer walls.

6. Isothermal tube wall surface with the persistent heat flux on the annular surface.

3.4 Governing Equation

The equations that govern the heat transfer and fluid motion in the tube and shell that Cylindrical-polar coordinates (r–θ–z) are:

3.4.1 Continuity, momentum and energy equations.

Continuity Equation

$$\frac{1}{r}\frac{\partial(rv_r)}{\partial r} + \frac{1}{r}\frac{\partial(v_\theta)}{\partial\theta} + \frac{\partial(v_z)}{\partial z} = 0 \text{------------------------(3.1)}$$

Momentum Equation

r- Direction

$$v_r\frac{\partial v_r}{\partial r} + \frac{v_\theta}{r}\frac{\partial v_r}{\partial\theta} + v_z\frac{\partial v_r}{\partial r} - \frac{v_\theta^2}{r} = -\frac{1}{\rho}\frac{\partial p}{\partial r} + \frac{\mu}{\rho}\left(\frac{1}{r}\frac{\partial}{\partial r}\left(r\frac{\partial v_r}{\partial r}\right) + \frac{1}{r^2}\frac{\partial^2 v_r}{\partial\theta^2} + \frac{\partial^2 v_r}{\partial z^2} - \frac{v_r}{r^2} - \frac{2}{r^2}\frac{\partial v_\theta}{\partial\theta}\right)$$

$$\text{------------------------------------(3.2)}$$

θ-Direction

$$v_r\frac{\partial v_\theta}{\partial r} + \frac{v_\theta}{r}\frac{\partial v_\theta}{\partial\theta} + v_z\frac{\partial v_\theta}{\partial r} + \frac{v_r v_\theta}{r} = -\frac{1}{\rho}\frac{\partial p}{\partial\theta} + \frac{\mu}{\rho}\left(\frac{1}{r}\frac{\partial}{\partial r}\left(r\frac{\partial v_\theta}{\partial r}\right) + \frac{1}{r^2}\frac{\partial^2 v_\theta}{\partial\theta^2} + \frac{\partial^2 v_\theta}{\partial z^2} - \frac{v_\theta}{r^2} + \frac{2}{r^2}\frac{\partial v_r}{\partial\theta}\right)$$

$$\text{---(3.3)}$$

Z-Direction

$$v_r\frac{\partial v_z}{\partial r} + \frac{v_\theta}{r}\frac{\partial v_z}{\partial\theta} + v_z\frac{\partial v_z}{\partial z} = -\frac{1}{\rho}\frac{\partial p}{\partial z} + \frac{\mu}{\rho}\left(\frac{1}{r}\frac{\partial}{\partial r}\left(r\frac{\partial v_z}{\partial r}\right) + \frac{1}{r^2}\frac{\partial^2 v_z}{\partial\theta^2} + \frac{\partial^2 v_z}{\partial z^2}\right)\text{----------------}$$

$$\text{---(3.4)}$$

Energy Equation

$$\rho c_p\left(v_r\frac{\partial T}{\partial r} + \frac{v_\theta}{r}\frac{\partial T}{\partial\theta} + v_z\frac{\partial T}{\partial z}\right) = k\left(\frac{\partial^2 T}{\partial r^2} + \frac{1}{r}\frac{\partial T}{\partial r} + \frac{1}{r^2}\frac{\partial^2 T}{\partial\theta^2} + \frac{\partial^2 T}{\partial z^2}\right)\text{-----------------}$$

$$\text{---(3.5)}$$

3.4.2 Reynolds-Averaged Navier-Stokes (RANS)

RANS equations in tensor notation are shown by (the over bar on the mean velocity is released).

$$\frac{\partial r}{\partial t} + \frac{\partial r U_i}{\partial x_i} = 0 \text{ --(3.6)}$$

$$\frac{\partial_i}{\partial t}(r u_i) + \frac{\partial u}{\partial x_j}(r u_i u_j) = -\frac{\partial P}{\partial x_i} + \frac{\partial}{\partial x_i}\left[m\left(\frac{\partial u_i}{\partial x_j} + \frac{\partial u_j}{\partial x_i} - \frac{2}{3} d_{ij} \frac{\partial u_i}{\partial x_i} \right) \right] + \frac{\partial}{\partial x_j}\left(\overline{r u'_i u'_j} \right)$$

---(3.7)

By time-averaging the instantaneous Navier-Stokes equation, additional terms perform that represents the influence of turbulence. These are the Reynolds stresses, $\overline{r u'_i u'_j}$.

3.4.3 Two Equations Turbulence Models

The turbulence model contains two equations which used for solving the two transport equations and symbolize the turbulent characteristics and get the eddy viscosity. This permits the models in order to account the impacts of special history such as the turbulent energy diffusion and convection. The variables of transport consists of two variables which are the turbulent kinetic energy k and the specific dissipation ε for k-ε model. The first variable of transport defines the turbulence energy whereas the second variable defines the turbulence scale. it is defined as: Rajesh **2013 [36].**

$$\frac{\partial(\rho k)}{\partial t} + \frac{\partial}{\partial xj}(\rho Ujk) = \frac{\partial}{\partial xj}\left[\left(\mu + \frac{\mu_t}{\sigma_k}\right)\frac{\partial k}{\partial xj}\right] + P_k - \rho\varepsilon + P_{kb}$$------------(3.8)

$$\frac{\partial(\rho\varepsilon)}{\partial t} + \frac{\partial}{\partial xj}(\rho Uj\varepsilon) = \frac{\partial}{\partial xj}\left[\left(\mu + \frac{\mu_t}{\sigma_\varepsilon}\right)\frac{\partial\varepsilon}{\partial xj}\right] + \frac{\varepsilon}{k}(c_{\varepsilon 1}P_k - c_{\varepsilon 2}\rho\varepsilon + c_{\varepsilon 3}P_{\varepsilon b})$$ ------------------

--(3.9)

Where $C_{\varepsilon 1}$=1.44, $C_{\varepsilon 2}$ =1.92   and σ_k =1

And P_{kb} and $P_{\varepsilon b}$ represent the effect of the buoyancy forces. P_k is the turbulence construction due to viscous forces, that modeled by:

$$P_k = \mu_t\left(\frac{\partial v_i}{\partial x_j} + \frac{\partial v_j}{\partial x_i}\right)\frac{\partial v_i}{\partial x_j} - \frac{2}{3}\frac{\partial v_k}{\partial x_k}\left(3\mu_t\frac{\partial v_k}{\partial x_k} + \rho k\right)$$--------------------(3.10)

The K-ε model take up that the viscosity of turbulence is related to the kinetic energy of turbulence and dissipation through the relation. **Rajesh 2013 [36]**:

$$\mu_t = C_\mu\rho\frac{k^2}{\varepsilon}$$ --(3.11)

Where C_μ =0.09

3.5   Mesh Generation

3.5.1   Three Dimensional Mesh Generation

The structured and unstructured volume meshing includes two types of methods. The integral form of governing equations is discredited using finite-volume. A structured grid was used in the present work for all models, the wall thickness it not considered for the outer shell. The generation mesh for the present models is shown in figures (3.2) and (3.3).
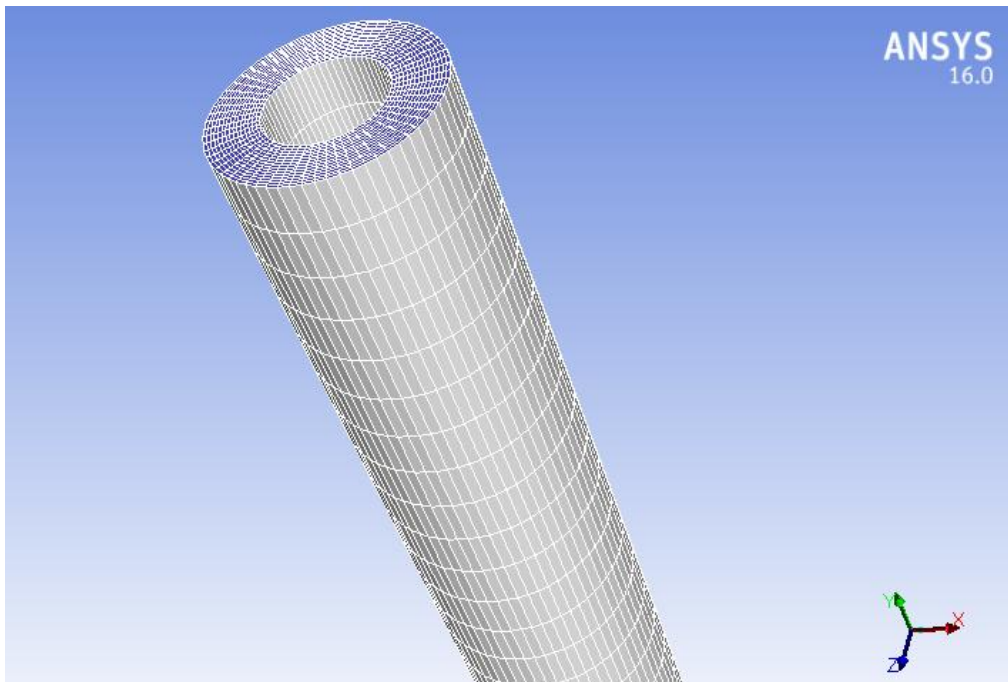

Figure 3.2 Mesh generation of straight annular model
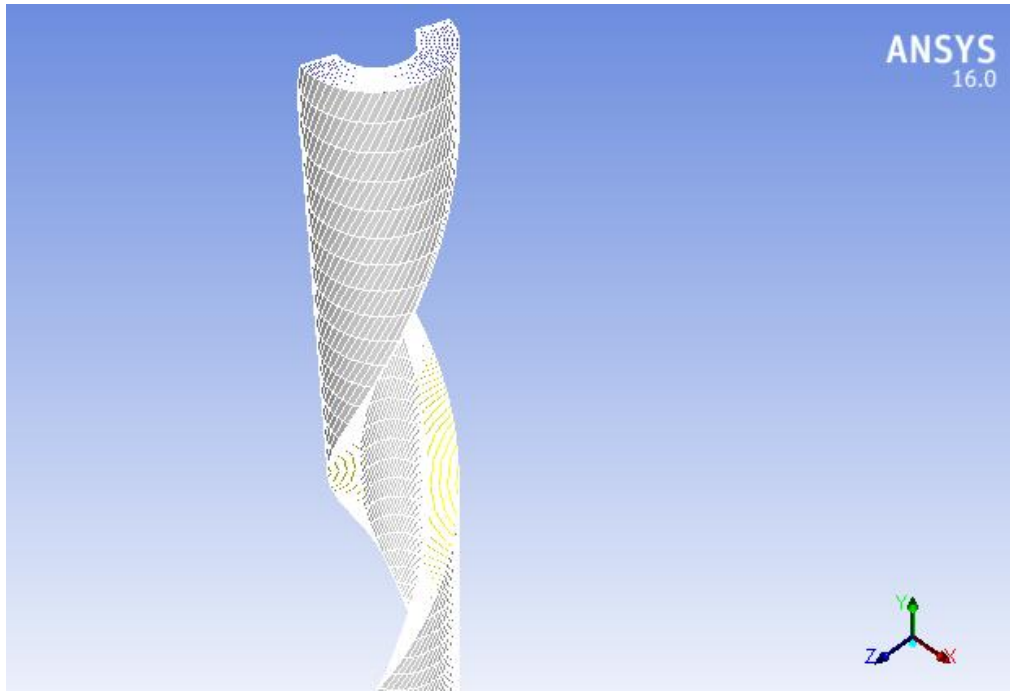
Figure 3.3 Mesh generation of twist annular model

3.5.2 Mesh Dependency

In order to determine if the solution is determined by the grid independent or no, can be determined by creating a grid with more cells and compare the solutions model. The tests of grid refinement for the temperature of average static on hot surface specified that the grid size of nearly (131822 cell) for the straight annular model and (123511 cell). The straight model is validated against experimental results in chapter 4. For the twist case, no experimental results are available at the current time so mesh dependency test is carried out as in table (3.2).

Table 3.2 Mesh dependency study for Twist at Re=5000.

Mesh type	Number of nodes	Nu
Coarse mesh	50114	105.42
Medium mesh	85486	108.80
Fine mesh	132056	111.86
more fine mesh	262189	112.22

From the results in Table 3.2, we notice that the value for Nu number changes only by 0.3% after the fine mesh. This means that the fine mesh can be used for the investigations and it will provide sufficient accuracy and resolution to be adopted.

y+ value for Re (500) = 4.5 and for Re (6000) = 3.7

3.6   Boundary conditions

In the three dimensions numerical investigations a correct definition of boundary conditions are even more difficult than it in the one dimension. The boundary condition of inlet, outlet, and solid walls are necessary for calculating the flow characteristics through the test section. The models in the present work considers as four cases with turbulent flow in the annular regime.The boundary conditions specifications for all cases are given in tables (3.3) to (3.6) specification of preliminary and periphery circumstances for straight annular with air fluid flow.

Table 3.3 Specification of initial and boundary conditions for straight annular with air fluid flow.

Reynolds Number	Inlet Temperature (K^o)	Temperature wall (K^o)	Air density (kg/m^3)	Air viscosity (kg/m.s)	Fluid annular flow velocity (m/s)
500	300	473	1.225	$1.79*10^{-5}$	0.365184
1000	300	473	1.225	$1.79*10^{-5}$	0.730367
1500	300	473	1.225	$1.79*10^{-5}$	1.095551
2000	300	473	1.225	$1.79*10^{-5}$	1.460735
2500	300	473	1.225	$1.79*10^{-5}$	1.825918
3000	300	473	1.225	$1.79*10^{-5}$	2.191102
3500	300	473	1.225	$1.79*10^{-5}$	2.556286
4000	300	473	1.225	$1.79*10^{-5}$	2.921469
4500	300	473	1.225	$1.79*10^{-5}$	3.286653
5000	300	473	1.225	$1.79*10^{-5}$	3.651837
5500	300	473	1.225	$1.79*10^{-5}$	4.01702
6000	300	473	1.225	$1.79*10^{-5}$	4.382204

Table 3.4 Specification of initial and boundary conditions for straight annular with water fluid flow

Reynolds Number	Inlet Temperature (K^o)	Temperature wall (K^o)	Water density (kg/m^3)	Water viscosity (kg/m.s)	Fluid annular flow velocity (m/s)
500	300	473	998.2	0.001003	0.02512
1000	300	473	998.2	0.001003	0.05024
1500	300	473	998.2	0.001003	0.075361
2000	300	473	998.2	0.001003	0.100481
2500	300	473	998.2	0.001003	0.125601
3000	300	473	998.2	0.001003	0.150721
3500	300	473	998.2	0.001003	0.175842
4000	300	473	998.2	0.001003	0.200962
4500	300	473	998.2	0.001003	0.226082
5000	300	473	998.2	0.001003	0.251202
5500	300	473	998.2	0.001003	0.276322
6000	300	473	998.2	0.001003	0.301443

Table 3.5 Specification of initial and boundary conditions for twist annular with air fluid flow

Reynolds Number	Inlet Temperature (K^o)	Temperature wall (K^o)	Air density (kg/m^3)	Air viscosity (kg/m.s)	Fluid annular flow velocity (m/s)
500	300	473	1.225	$1.79*10^{-5}$	0.365184
1000	300	473	1.225	$1.79*10^{-5}$	0.730367
1500	300	473	1.225	$1.79*10^{-5}$	1.095551
2000	300	473	1.225	$1.79*10^{-5}$	1.460735
2500	300	473	1.225	$1.79*10^{-5}$	1.825918
3000	300	473	1.225	$1.79*10^{-5}$	2.191102
3500	300	473	1.225	$1.79*10^{-5}$	2.556286
4000	300	473	1.225	$1.79*10^{-5}$	2.921469
4500	300	473	1.225	$1.79*10^{-5}$	3.286653
5000	300	473	1.225	$1.79*10^{-5}$	3.651837
5500	300	473	1.225	$1.79*10^{-5}$	4.01702
6000	300	473	1.225	$1.79*10^{-5}$	4.382204

Table 3.6 Specification of initial and boundary conditions for twist annular with water fluid flow

Reynolds Number	Inlet Temperature (K^o)	Temperature wall (K^o)	Water density (kg/m^3)	Water viscosity (kg/m.s)	Fluid annular flow velocity (m/s)
500	300	473	998.2	0.001003	0.02512
1000	300	473	998.2	0.001003	0.05024
1500	300	473	998.2	0.001003	0.075361
2000	300	473	998.2	0.001003	0.100481
2500	300	473	998.2	0.001003	0.125601
3000	300	473	998.2	0.001003	0.150721
3500	300	473	998.2	0.001003	0.175842
4000	300	473	998.2	0.001003	0.200962
4500	300	473	998.2	0.001003	0.226082
5000	300	473	998.2	0.001003	0.251202
5500	300	473	998.2	0.001003	0.276322
6000	300	473	998.2	0.001003	0.301443

3.7   Initial Condition

The flow field can be determined only if the iteration is started. Thus, in order to start the solution, a preliminary estimate is needed.

If the preliminary circumstances are poor, it may result in divergence or at least lead to converge. At the current study, the whole variables are started from the boundary conditions.

The value of the velocity for each model are given in the tables (3.3)to (3.6) these values used to calculate the values of k and ϵ by the equation below **Rajesh 2013 [36].**

$$k = \frac{2}{3}(VI_{tur})^2 \text{--(3.12)}$$

when V is the mean primary velocity flow

$$\varepsilon = C_\mu^{3/4} \frac{k^{3/2}}{l} \text{--(3.13)}$$

$$I_{tur} = 0.16(R_e)^{-1/8} \text{--(3.14)}$$

Where C_μ is a turbulence model continuous which typically has a value of 0.09 and (ι) is the viscosity ratio.

3.8 Number of Iteration

The supreme number of repetitions used to reach a converged solution.

3.9 Convergence Criteria

This is the remaining values group under which, when the average residuals decrease, the solver will be ended itself. Residuals are the calculation errors. It is recognized that when the residuals for flow, comprising permanency and momentum parameters fall below 1×10^{-5}.

3.10 Contribution of this work

In this work four cases were modeled and solved using ANSYS bench package version **16.0**. Work included geometry generation using Pointwise program, then mesh using structure mesh. Boundary conditions were then set. Flow was solved for choosing number of iteration until convergence.

Chapter Four

Results and Discussion

4.1 Introduction

At this chapter, we will present the results obtained from the numerical solution by using the ANSYS – FLUENT Version 16 computer program, which was equipped for this aim. All the analysis was executed at two stages. The first stage for straight annular regime and the second stage for twist annular regime. Both of the stages are conducted with air and water as fluid flow in the annular regime for variable Reynolds Number namely of (500, 100, 1500, 2000, 2500, 3000, 3500, 4000, 4500, 5000, 5500, 6000).

4.2 Case Study

In 2015, [37] Hamed Sadighi Dizaji et al. Have conducted experimental analysis about the" The experimental studies on the properties of pressure drop and heat transfer for new provisions of corrugated tubes in a heat exchanger with double pipe ". Tube geometry is [$L_{(inner)}$ = 346mm, $D_{(ave)}$ = 85mm, $L_{(outer)}$ = 346mm, $D_{(ave)}$ = 106mm], D_h = 21mm, and 2r = 25.4mm.

Figure (4.1) shows the mesh generation and geometry of the case study.
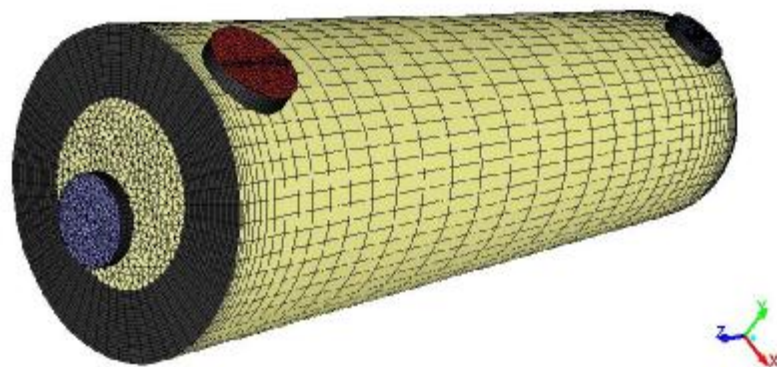
Figure 4.1 Geometry and mesh generation of the case study.

In Figures (4.2) and (4.3), shows a comparison of the case study between experimental results and numerical results, which included relationship between Reynolds number versus Nusselt number and friction factor. It can be observed that the Nusselt number and friction factor of numerical study are higher than the Nusselt number friction factor of experimental study for all Reynolds number. It can be shown that the numerical study increasing 2.9% and 2.3% respectively compared with experimental study.
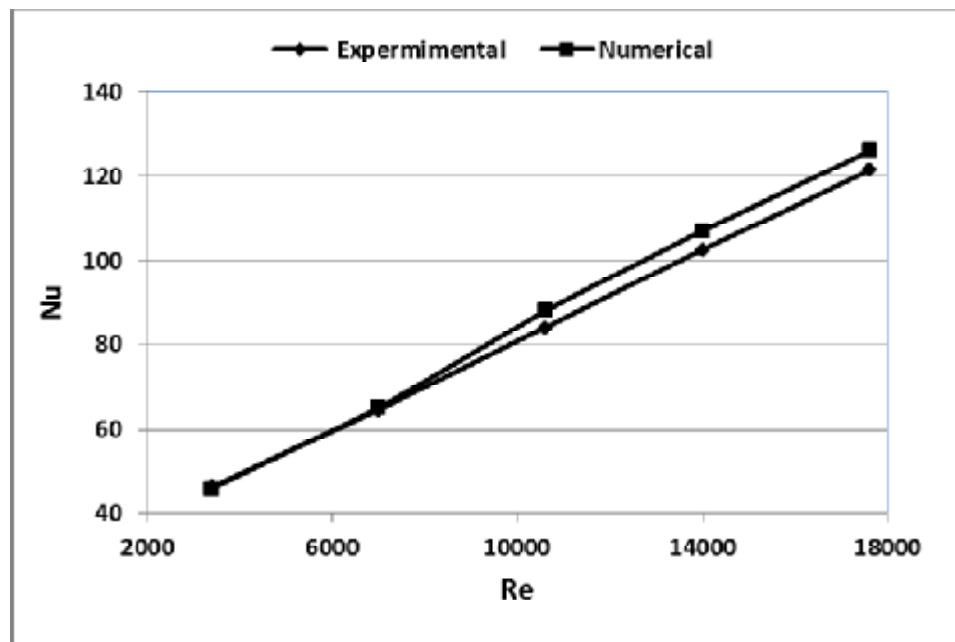
Figure 4.2 comparison of the case study between experimental results and numerical results for (Nu) versus (Re)
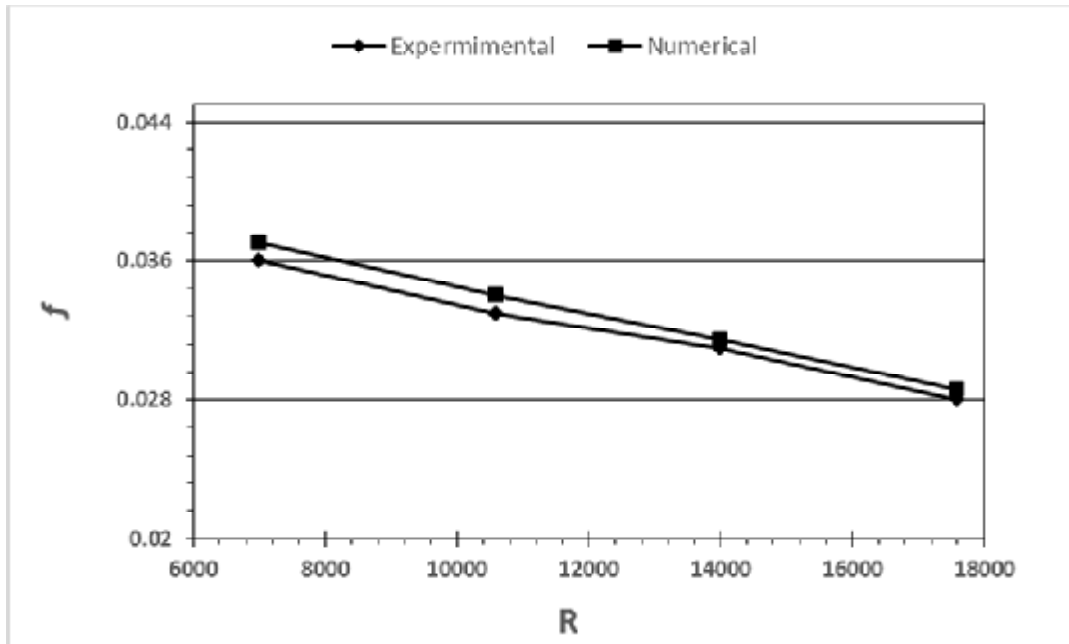
Figure 4.3 comparison of the case study between experimental results and numerical results for (f) versus (Re)

In table (4.1) and (4.2) shows the values of the friction element and Nusselt number for the experimental study with numerical study versus Reynolds number and error rate.

Table 4.1 detailing Nusselt number with Reynolds number.

Re	(Nu) Experimental	(Nu) Numerical	error
3400	46.5	46	1.075269
7000	64.5	65	0.775194
10600	84	88	4.761905
14000	102.5	107	4.390244
17600	121.5	126	3.703704
Average Error			2.941263 %

Table 4.2 detailing friction factor with Reynolds number.

Re	(f) Experimental	(f) Numerical	error
7000	0.036	0.037	2.777778
10600	0.033	0.034	3.030303
14000	0.031	0.0315	1.612903
17600	0.028	0.0286	2.142857
Average Error			2.39096%

4.3 Straight annular with air flow

The scaled residuals of the straight annular with air flow model found that the solution of model is converged at 200 iterations during 2 hour for Reynolds number of 5000 as shown in figure (4.4).
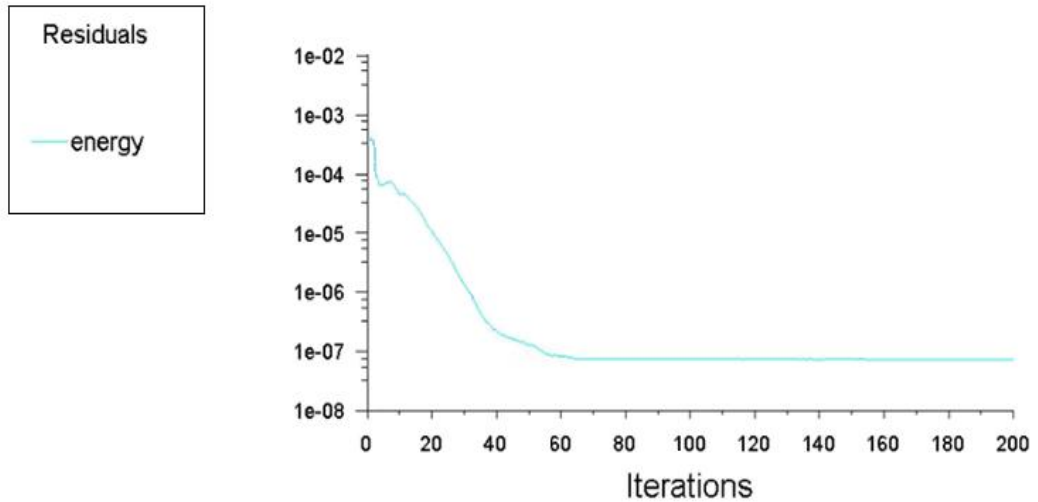
Figure 4.4 Scaled Residuals for Straight annular with air flow for Re=5000

Static temperature contour of the straight annular with air flow model for the case of Reynolds number of 5000 is shown in figure (4.5), the cross heat transfer impact in the straight shell area is observable from the temperature contour. It can be shown that the air temperature near inner tube is higher than air temperatures in the deeper shell side and there is symmetric distribution of air temperature due to constant heat flux and temperature of inner tube wall.
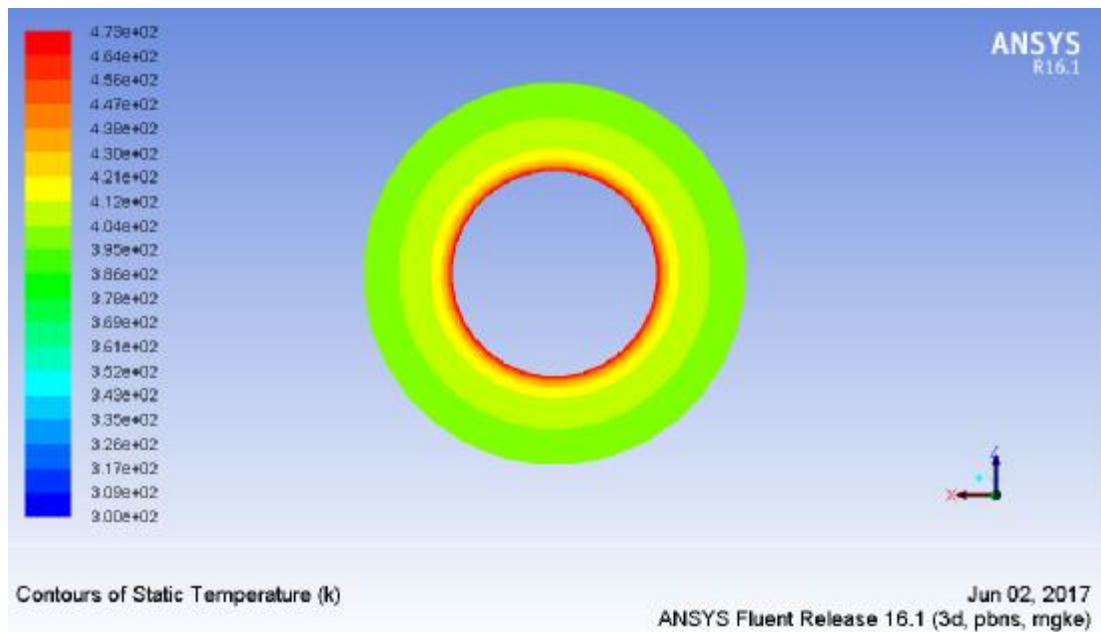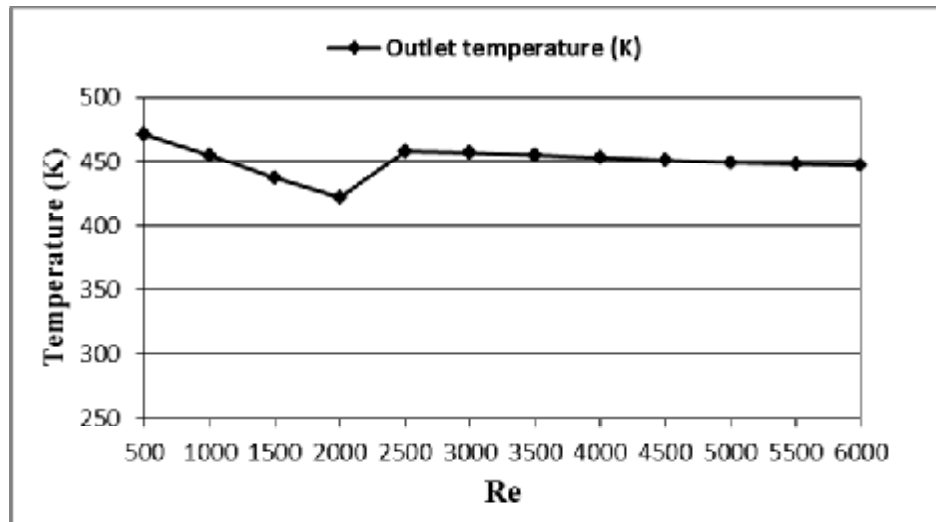
Figure 4.5 Outlet temperature contour for Straight annular with air flow for Re=5000

Figure (4.6) shows the relation between outlet temperatures of air in the shell side for Straight annular with air flow versus Reynolds number. The air outlet temperature is noticed to be variable values and decreased with Reynolds number increase. It is shown that the maximum and minimum outlet temperature is 470.7 K and 422.2 k at Reynolds number of 500 and 2000 respectively.

We notice that there are some discontinuities in the results. The reason behind those discontinuities is that the flow is laminar at Re number below 2000. After that transition occurs and finally the flow becomes fully turbulent at Re of 2500. However, In this study, turbulent solver was used in all the Re range.

Figure 4.6 Outlet temperature with Re for Straight annular with air flow

Figure (4.7) shows the relation between the inlet and outlet temperatures difference of air in the shell side for Straight annular with air flow versus Reynolds number. The temperatures differences of air are noticed to be variable values and decreased with increasing of Reynolds number. It is shown that the maximum and minimum temperature differences of air are 170.7 K and 122.2 k at Reynolds number of 500 and 2000 respectively.
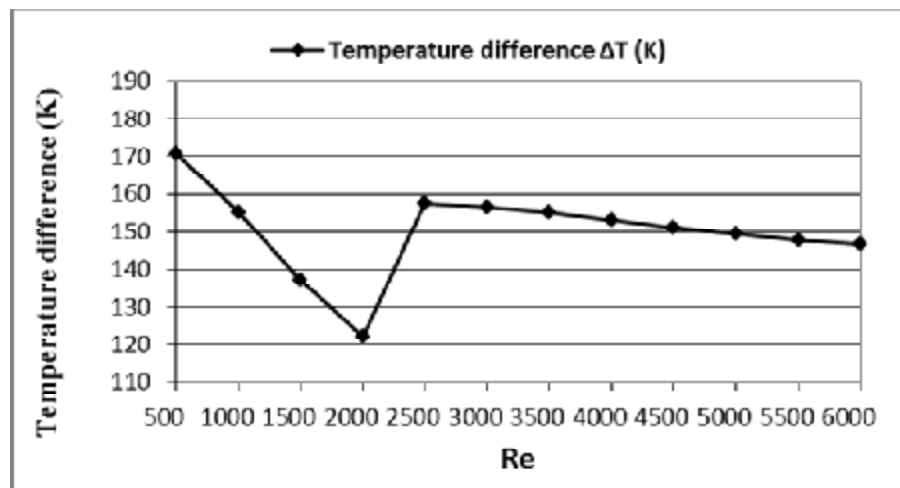
Figure 4.7 Inlet and outlet temperature difference with Re for Straight annular with air flow

Figure (4.8) shows the relation between heat fluxes from outer tube surface for Straight annular with air flow versus Reynolds number. The heat flux is noticed to be variable values and increased with increasing of Reynolds number. It can be shown that the maximum and minimum heat flux values are 2875.4 W/m^2 and 286.6 W/m^2 at Reynolds number of 6000 and 500 respectively.
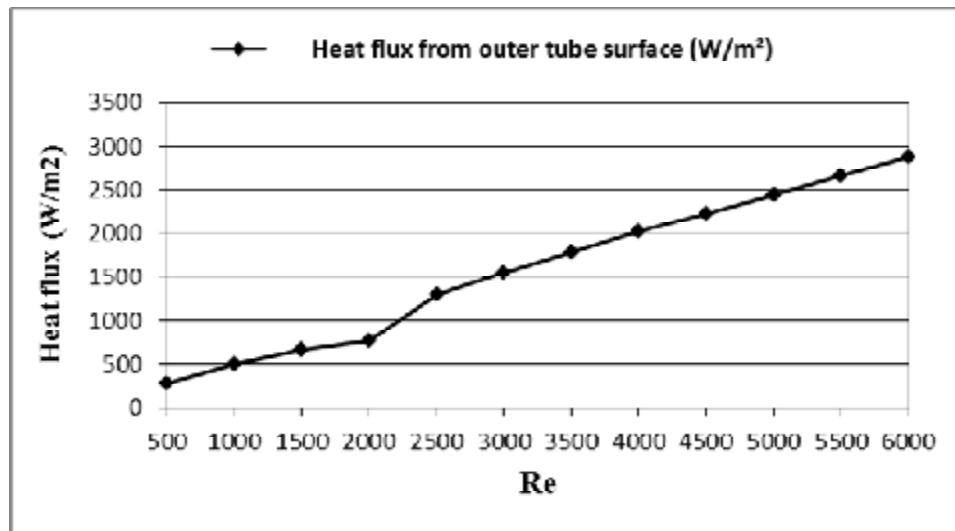
Figure 4.8 Heat flux with Re for Straight annular with air flow

Figure (4.9) shows the relation between Nusselt numbers of outer tube surface for Straight annular with air flow versus Reynolds number. The Nusselt number is observed to be variable values and increased with increasing of Reynolds number. In the turbulent flow the Nusselt number increased as Reynolds number increased because of increasing in turbulent concentration as Reynolds number increased. It can be shown that the minimum Nusselt number value is 2.7 occurs at Reynolds number of 500 and 27.3 occurs at Reynolds number of 6000.
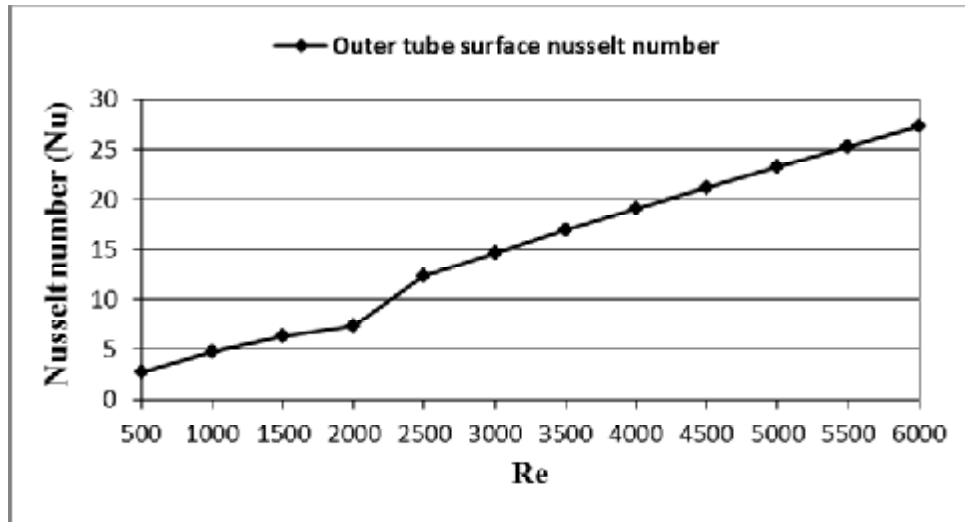
Figure 4.9 Nusselt number with Re for Straight annular with air flow

Figure (4.10) shows the relation between film heat transfer coefficients of outer tube surface for Straight annular with air flow versus Reynolds number. The factor of heat transfer is seen to be variable values and increased with increasing of Reynolds number. It can be shown that the minimum film heat transfer coefficients value is 3.3 W/m².K occurs at Reynolds number of 500 and 33 W/m².K arises at Reynolds number of 6000.
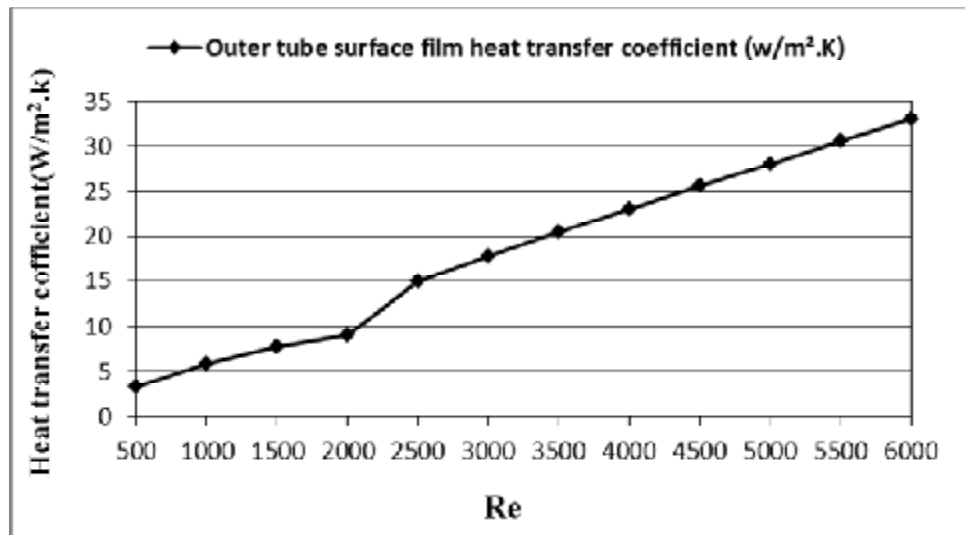
Figure 4.10 Film heat transfer coefficient with Re for Straight annular with air flow

Figure (4.11) shows the relation between pressure drops in shell side for Straight annular with air flow versus Reynolds number. The drop of pressure is noticed to be variable values and increased with increasing of Reynolds number due to increasing in air velocity. It can be shown that the maximum and minimum pressure drop values are 112 Pascal and 3 Pascal at Reynolds number of 6000 and 500 respectively.
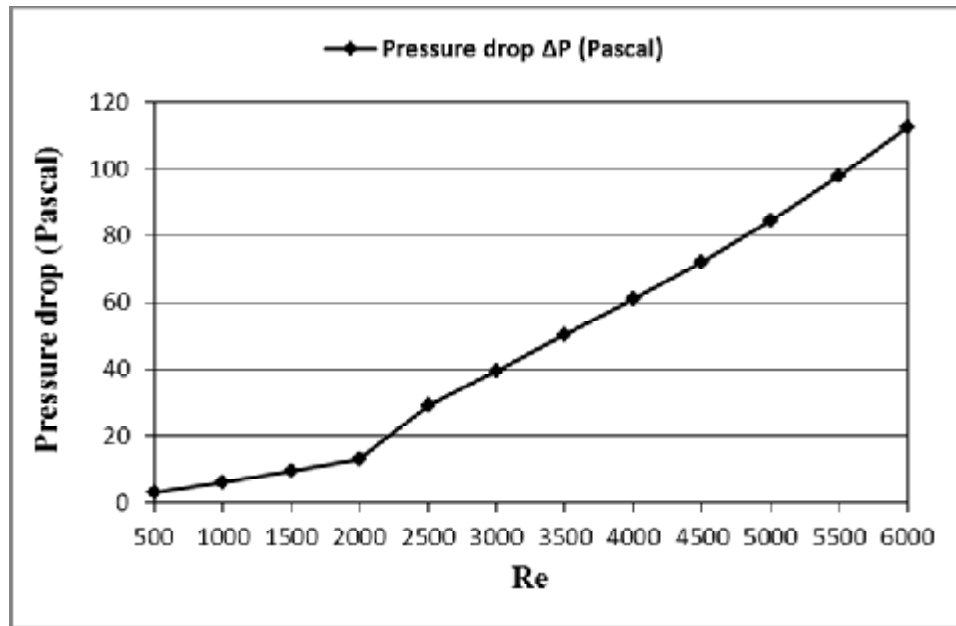

Figure 4.11 Pressure drop with Re for Straight annular with air flo

4.4   Straight annular with water flow

The scaled residuals of the straight annular with water flow model found that the solution of model is converged at 200 iterations during 2 hour for Reynolds number of 5000 as shown in figure (4.12)
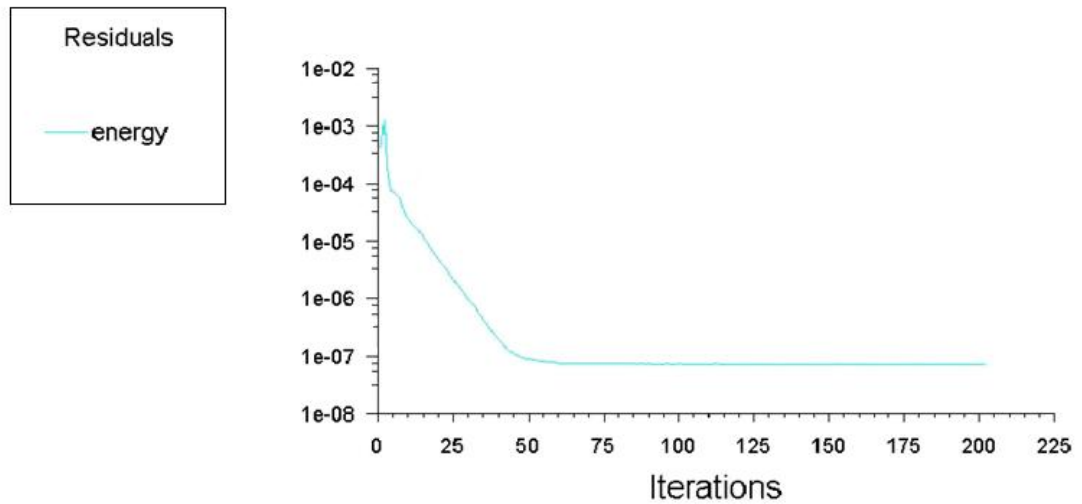
Figure 4.12 Scaled Residuals for Straight annular with water flow for Re=5000

Static temperature contour of the straight annular with water flow model for the case of Reynolds number of 5000 is shown in figure (4.13), the cross impact heat transfer in the straight shell area is observable from the contour of temperature. It can be shown that the water temperature near inner tube is higher than water temperatures in the deeper shell side and there is symmetric distribution of water temperature due to constant heat flux and temperature of inner tube wall.
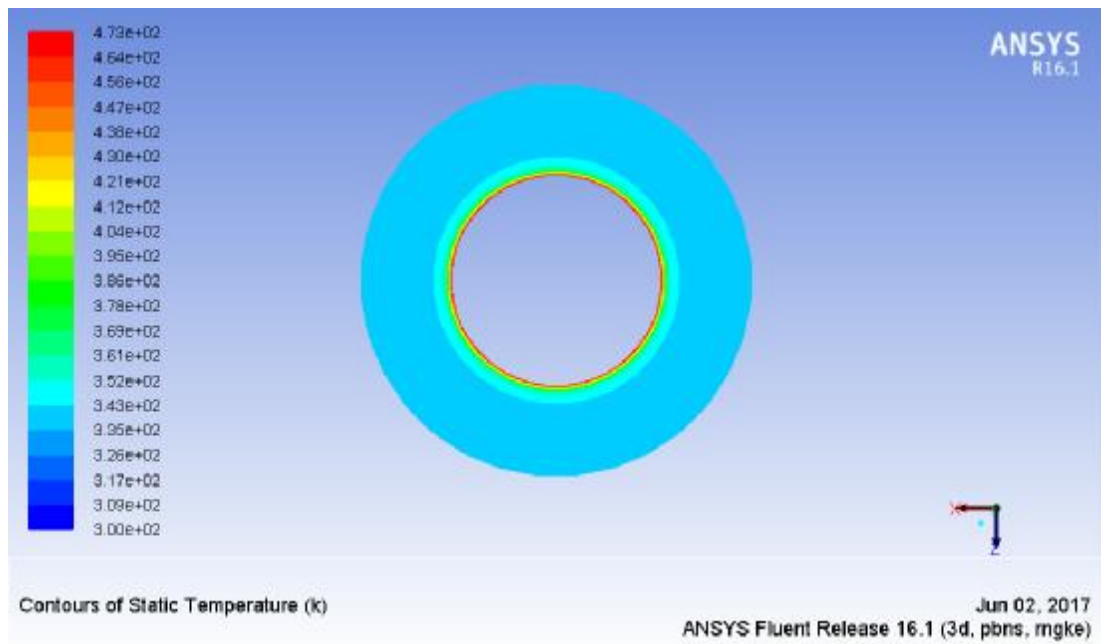
Figure 4.13 Outlet temperature contour for Straight annular with water flow for
Re=5000

Figure (4.14) shows the relation between outlet temperatures of water in the
shell side for Straight annular with water flow versus Reynolds number. The water
outlet temperature is noticed to be variable values and decreased with increasing of
Reynolds number.   It can be shown that the maximum and minimum outlet
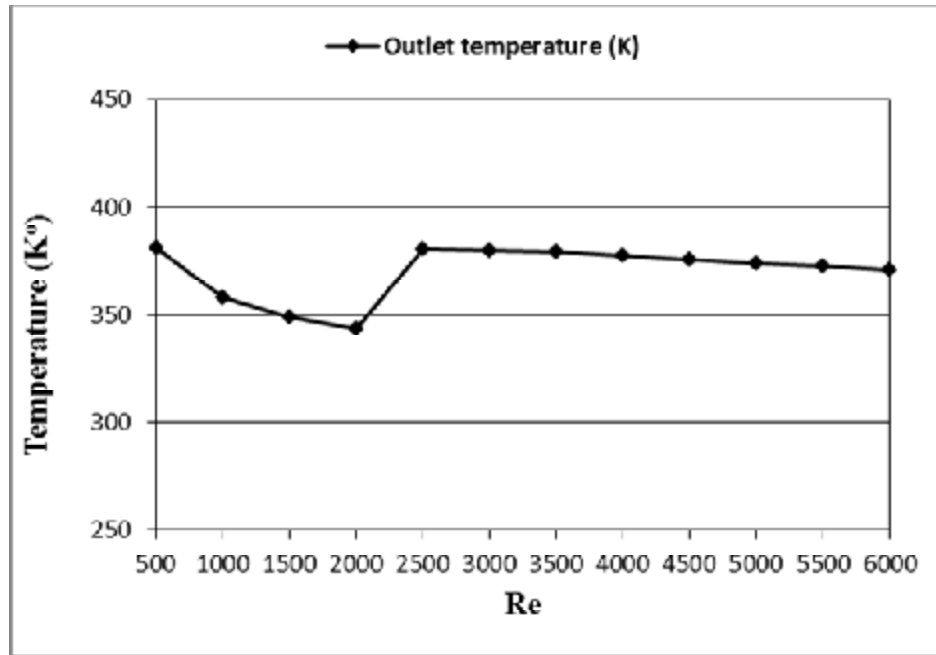temperature is 380 K and 343.5 k at Reynolds number of 500 and 2000 respectively.

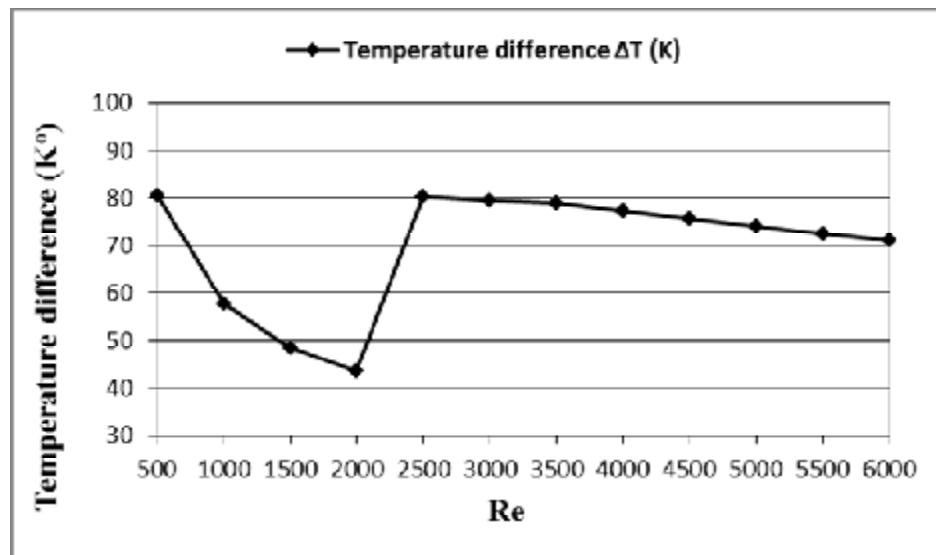Figure 4.14 Outlet temperature with Re for Straight annular with water flow

Figure (4.15) shows the relation between Inlet and outlet water temperatures difference in the shell side for Straight annular with water flow versus Reynolds number. The temperatures differences of water are noticed to be variable values and decreased with increasing of Reynolds number. It can be shown that the maximum and minimum temperature differences of water are 80.6 K and 43.5 K at Reynolds number of 500 and 2000 respectively.

Figure 4.15 Inlet and outlet temperature difference with Re for Straight annular with water flow

Figure (4.16) shows the relation between heat fluxes from outer tube surface for Straight annular with water flow versus Reynolds number. The heat flux is noticed to be variable values and increased with increasing of Reynolds number. It can be shown that the maximum and minimum heat flux values are 307122.6 W/m^2 and 27267.7W/m^2 at Reynolds number of 6000 and 500 respectively.
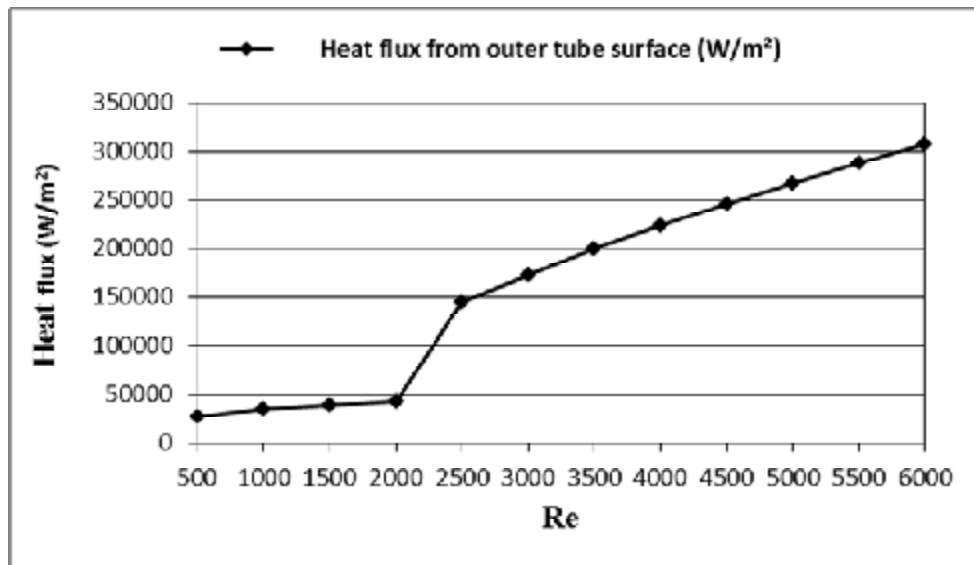

Figure 4.16 Heat flux with Re for Straight annular with water flow

Figure (4.17) shows the relation between Nusselt numbers of outer tube surface for Straight annular with water flow versus Reynolds number. The Nusselt number is observed to be variable values and increased with increasing of Reynolds number; in the turbulent flow the Nusselt number increased as Reynolds number increased because of increasing in turbulent strength as Reynolds number arised. It can be shown that the minimum Nusselt number value is 10.4 occurs at Reynolds number of 500 and 117.6 occurs at Reynolds number of 6000.
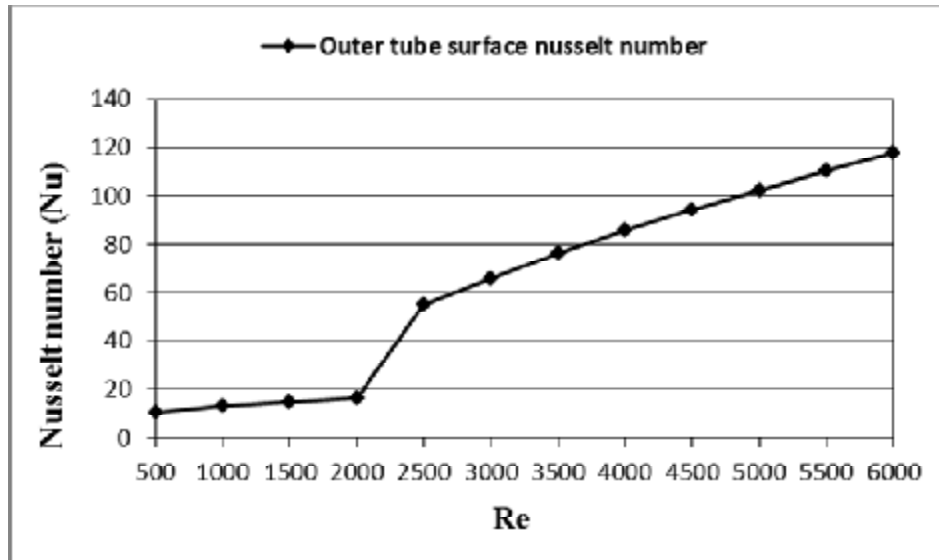
Figure 4.17 Nusselt number with Re for Straight annular with water Flow

Figure (4.18) shows the relation between film heat transfer coefficients of outer tube surface for Straight annular with water flow versus Reynolds number. The factor heat transfer is seen to be variable values and increased with increasing of Reynolds number. It can be shown that the minimum film heat transfer coefficients value is 313 W/m².K occurs at Reynolds number of 500 and 3530 W/m².K arises at Reynolds number of 6000.
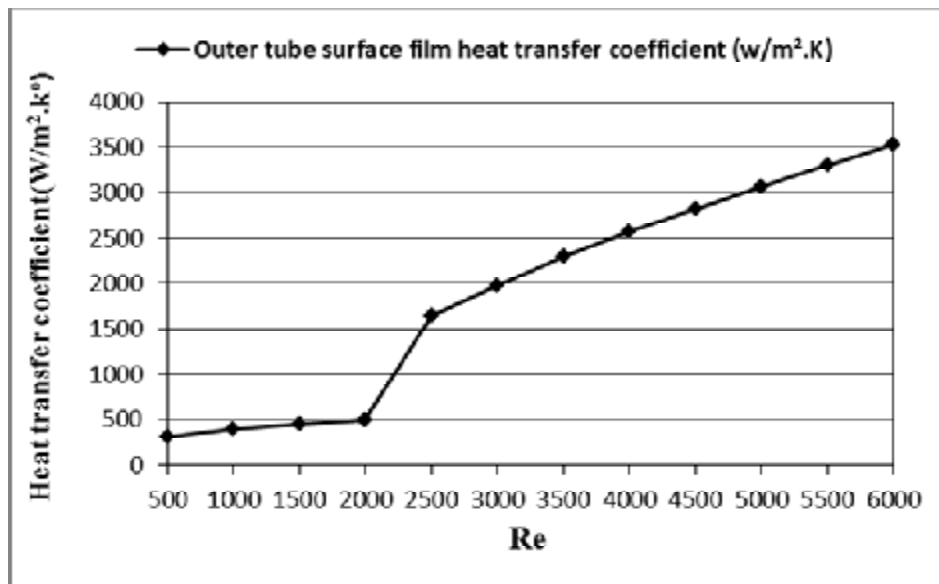
Figure 4.18 Heat transfer coefficient with Re for Straight annular with water flow

Figure (4.19) shows the relation between pressure drops in shell side for Straight annular with water flow versus Reynolds number. The drop of pressure is noticed to be variable values and increased with increasing of Reynolds number due to increasing in air velocity. It can be shown that the maximum and minimum pressure drop values are 112 Pascal and 433.4 Pascal at Reynolds number of 6000 and 500 respectively.
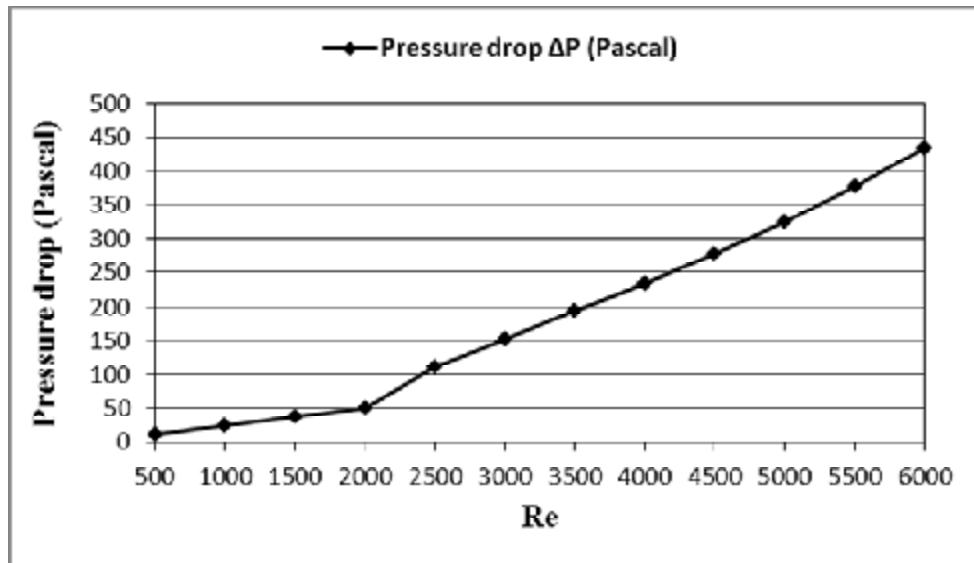

Figure 4.19 Pressure drop with Re for Straight annular with water flow

4.5   Twist annular with air flow

The scaled residuals of the twist annular with air flow model found that the solution of model is converged at 900 iterations during 6 hours for Reynolds number of 5000 as shown in figure (4.20).
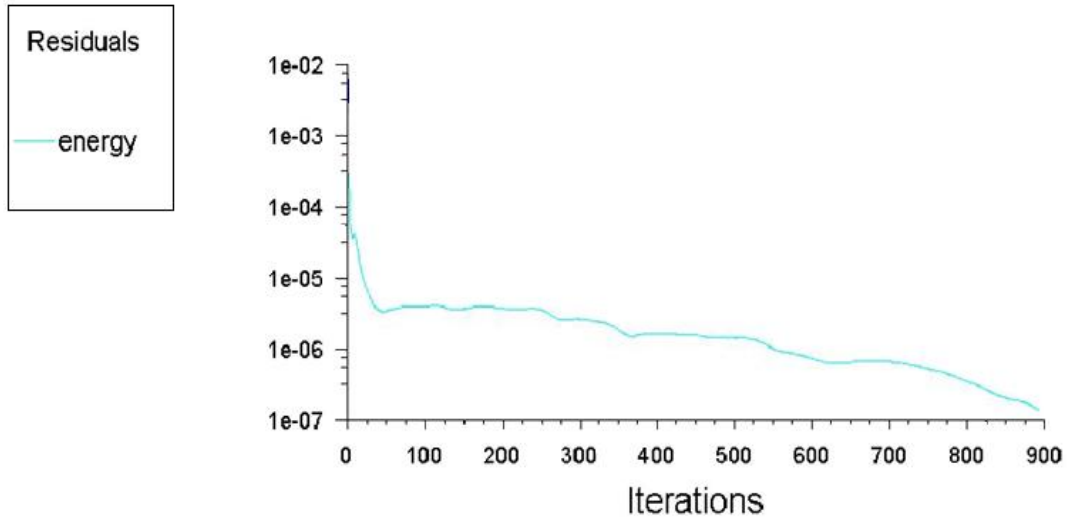

Figure 4.20 Scaled Residuals for twist annular with air flow for Re=5000

Static temperature contour of the twist annular with air flow model for the case of Reynolds number of 5000 is shown in figure (4.21), the cross impact heat transfer in the twist shell area is observable from the contour of temperature. It can be shown that the air temperature near inner tube is higher than air temperatures in the deeper shell side and there is no symmetric distribution of air temperature with constant heat flux and temperature of internal tube wall due twist flow in the shell regime.
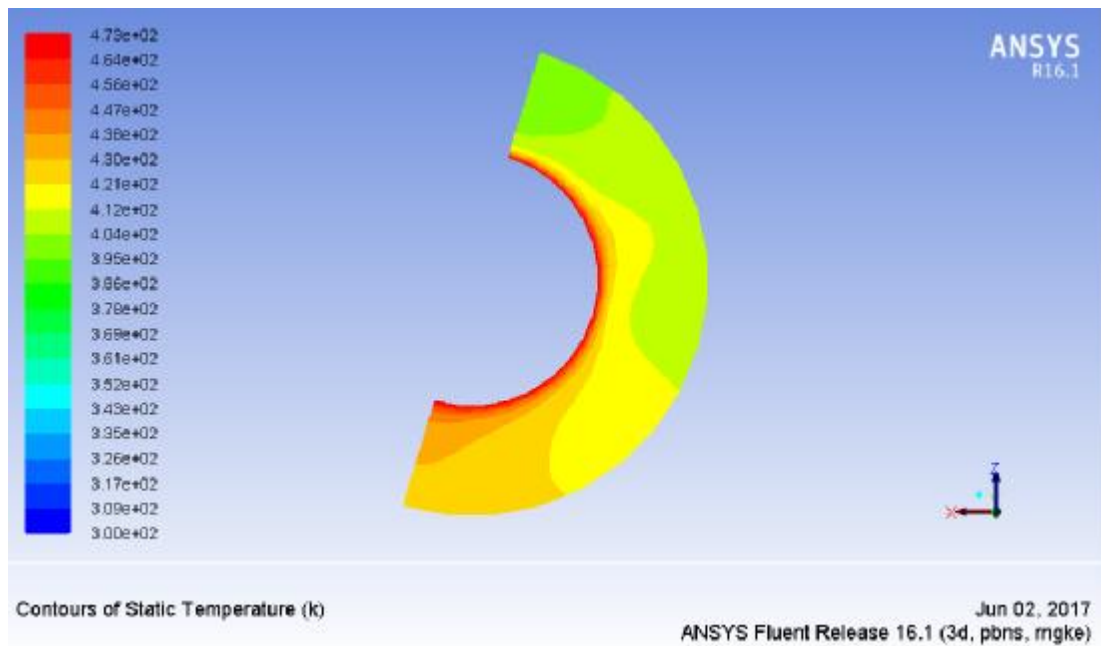
Figure 4.21 Outlet temperature contour for twist annular with air flow for Re=5000

Figure (4.22) shows the relation between outlet temperatures of air in the shell side for twist annular with air flow versus Reynolds number. The air outlet temperature is noticed to be variable and decreased with increasing of Reynolds number. It can be shown that the maximum and minimum outlet temperature is 472.8 K and 453.6 k at Reynolds number of 500 and 6000 respectively.
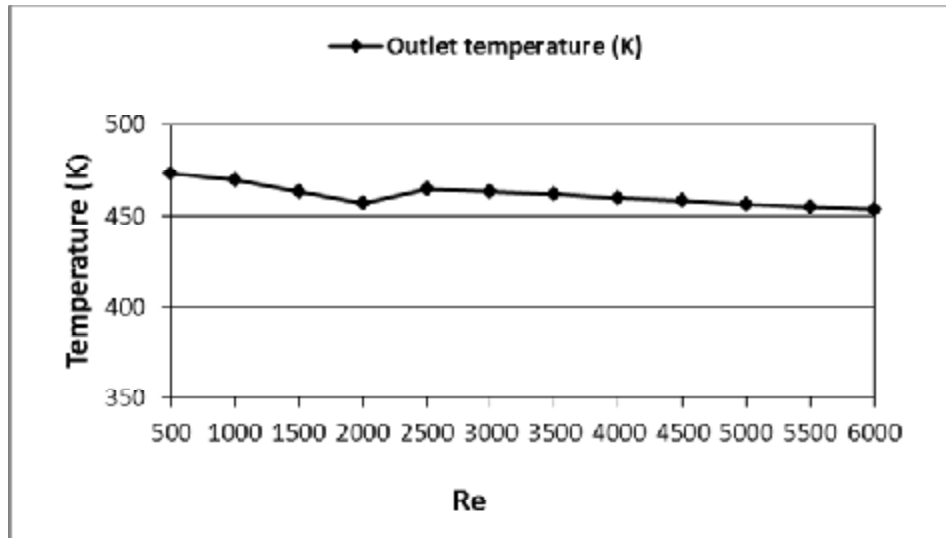
Figure 4.22 Outlet temperature with Re for twist annular with air flow

Figure (4.23) shows the relation between Inlet and outlet temperatures difference of air in the shell side for twist annular with air flow versus Reynolds number. The air temperatures differences of air are noticed to be variable values and decreased with increasing of Reynolds number. It can be shown that the maximum and minimum temperature differences of air are 172.8 K and 153.6 K at Reynolds number of 500 and 6000 respectively.
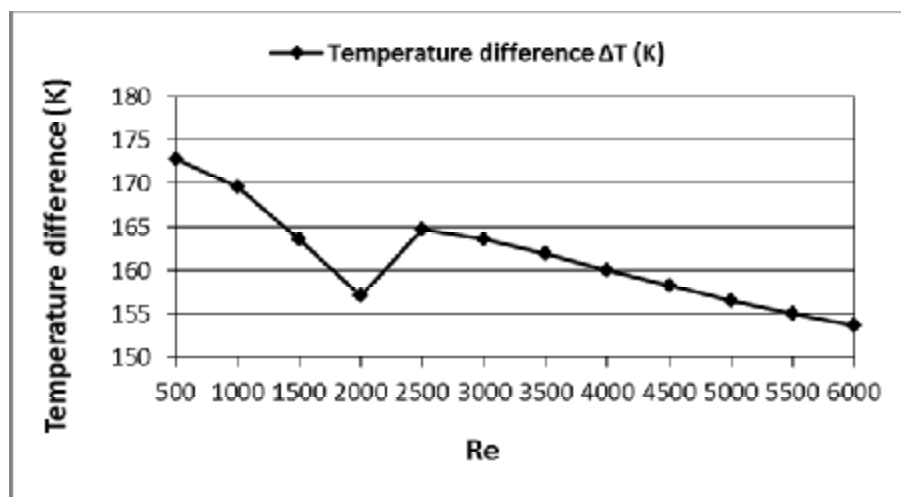

Figure 4.23 Inlet and outlet temperature difference with Re for twist annular with air flow

Figure (4.24) shows the relation between heat fluxes from outer tube surface for twist annular with air flow versus Reynolds number. The heat flux is noticed to be variable values and increased with increasing of Reynolds number. It can be shown that the maximum and minimum heat flux values are 3057.4 W/m^2 and 297.3 W/m^2 at Reynolds number of 6000 and 500 respectively.
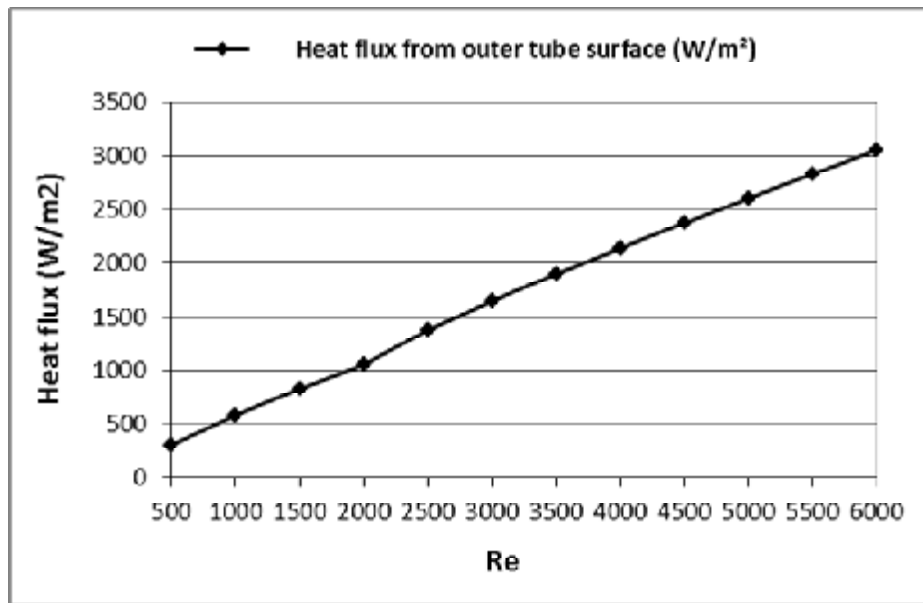

Figure 4.24 Heat flux with Re for twist annular with air flow

Figure (4.25) shows the relation between Nusselt numbers of outer tube surface for twist annular with air flow versus Reynolds number. The Nusselt number is observed to be variable values and increased with increasing of Reynolds number; in the turbulent flow the Nusselt number increased as Reynolds number increased because of increasing in turbulent intensity as Reynolds number increased. It is shown that the minimum Nusselt number value is 2.8 occurs at Reynolds number of 500 and 29 occurs at Reynolds number of 6000.
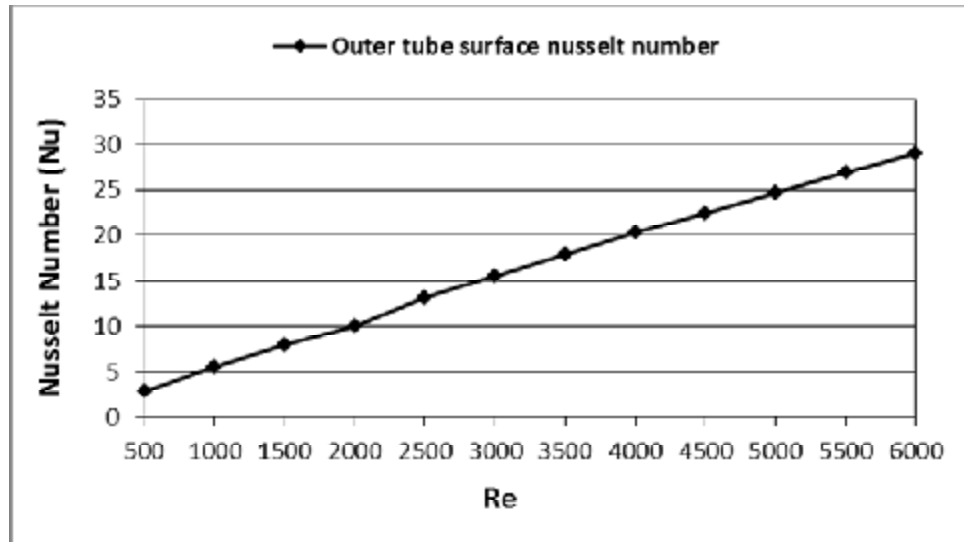
Figure 4.25 Nusselt number with Re for twist annular with air Flow

Figure (4.26) shows the relation between film heat transfer coefficients of outer tube surface for twist annular with air flow versus Reynolds number. The factor of heat transfer is seen to be variable values and increased with increasing of Reynolds number. It is shown that the minimum film heat transfer coefficients value is 3.4 occurs at Reynolds number of 500 and 35 occurs at Reynolds number of 6000.
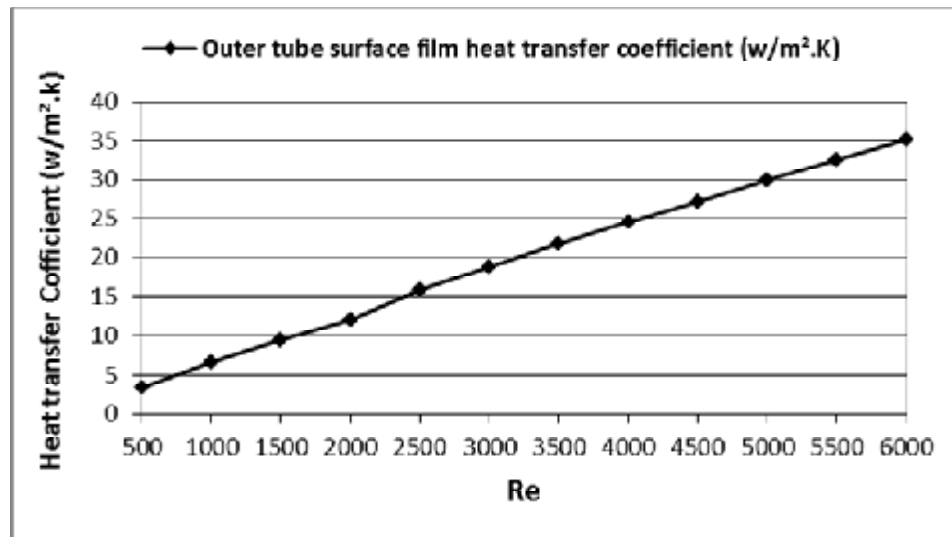

Figure 4.26 Heat transfer coefficient with Re for twist annular with air flow

Figure (4.27) shows the relation between pressure drops in shell side for twist annular with air flow versus Reynolds number. The drop of pressure is noticed to be variable values and increased with increasing of Reynolds number due to increasing in air velocity. It can be shown that the maximum and minimum pressure drop values are 145 Pascal and 4 Pascal at Reynolds number of 6000 and 500 respectively.
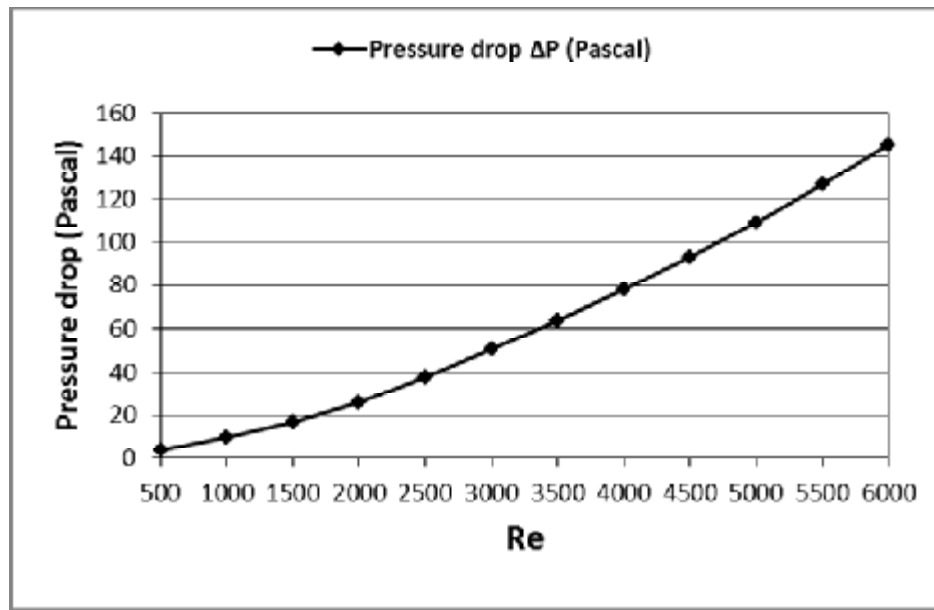

Figure 4.27 Pressure drop with Re for twist annular with air flow

4.6 Twist annular with water flow

The scaled residuals of the twist annular with water flow model found that the solution of model is converged at 900 iterations during 6 hours for Reynolds number of 5000 as shown in figure (4.28)
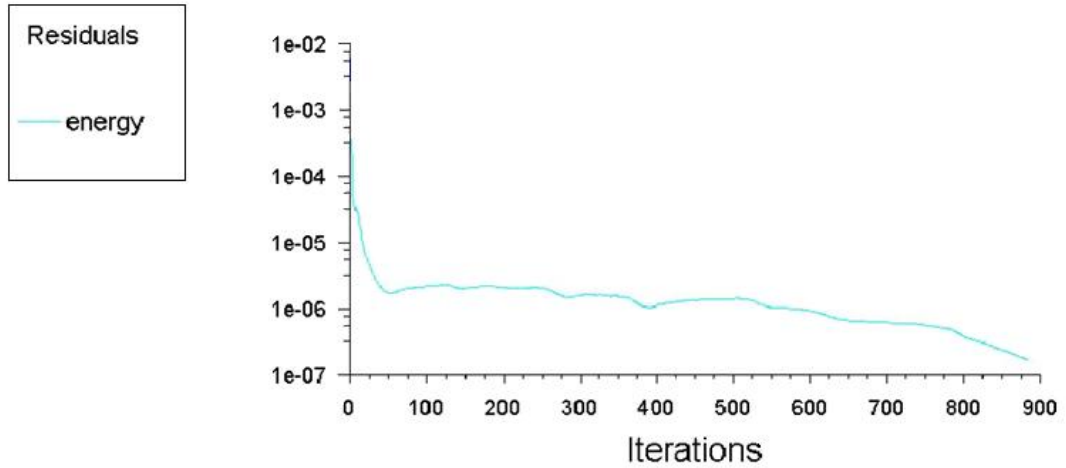

Figure 4.28 Scaled Residuals for twist annular with water flow for Re=5000

Static temperature contour of the twist annular with water flow model for the case of Reynolds number of 5000 is shown in figure (4.29), the cross impact heat transfer in the straight shell area is observable from the contour of temperature. It can be shown that the water temperature near inner tube is higher than water temperatures in the deeper shell side and there is no symmetric distribution of water temperature with constant heat flux and temperature of inner tube wall due to twist flow.
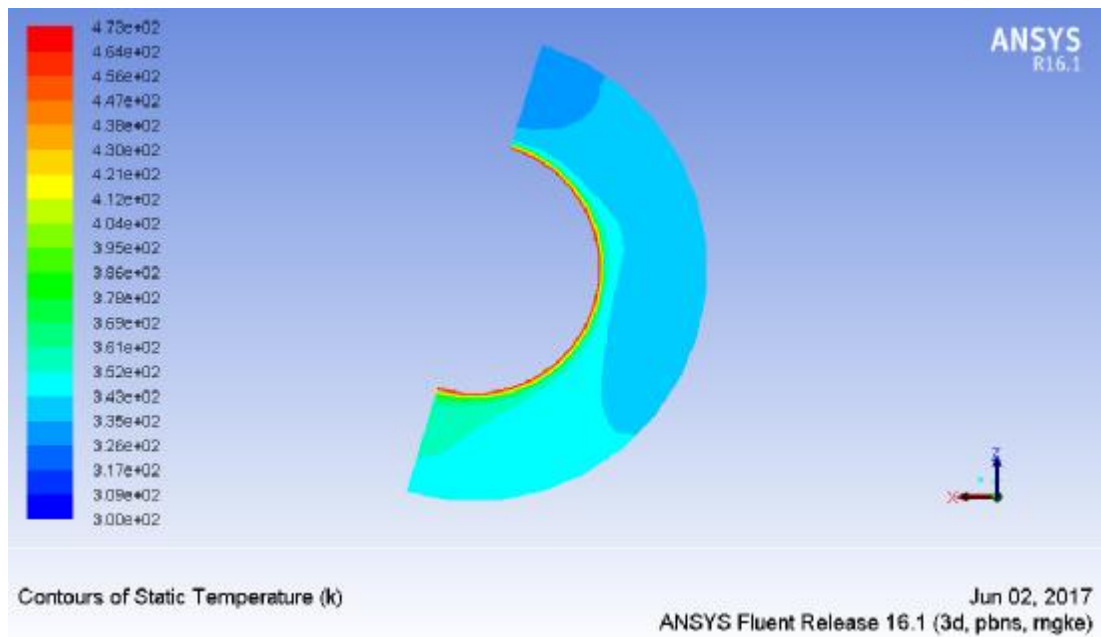
Figure 4.29 Outlet temperature contour for twist annular with water flow for Re=5000

Figure (4.30) shows the relation between outlet temperatures of water in the shell side for twist annular with water flow versus Reynolds number. The water outlet temperature is noticed to be variable and decreased with increasing of Reynolds number. It can be shown that the maximum and minimum outlet temperature is 426.7 K and 373.2 k at Reynolds number of 500 and 2000 respectively.
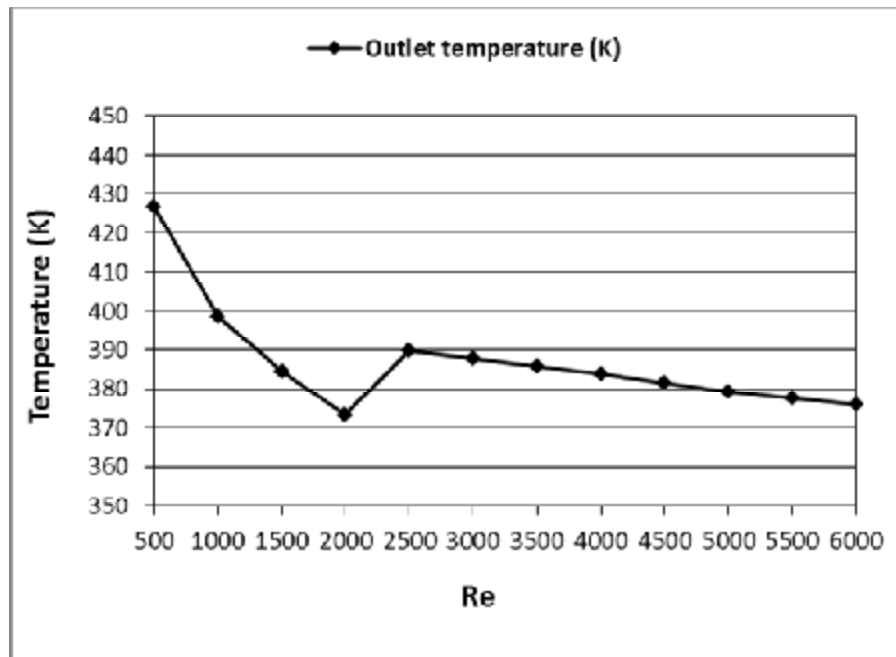
Figure 4.30 Outlet temperature with Re for twist annular with water flow

Figure (4.31) shows the relation between Inlet and outlet temperatures difference of water in the shell side for twist annular with water flow versus Reynolds number. The temperatures differences of water are noticed to be variable values and decreased with increasing of Reynolds number. It can be shown that the maximum and minimum temperature differences of water are 126.7 K and 73.3 K at Reynolds number of 500 and 2000 respectively.
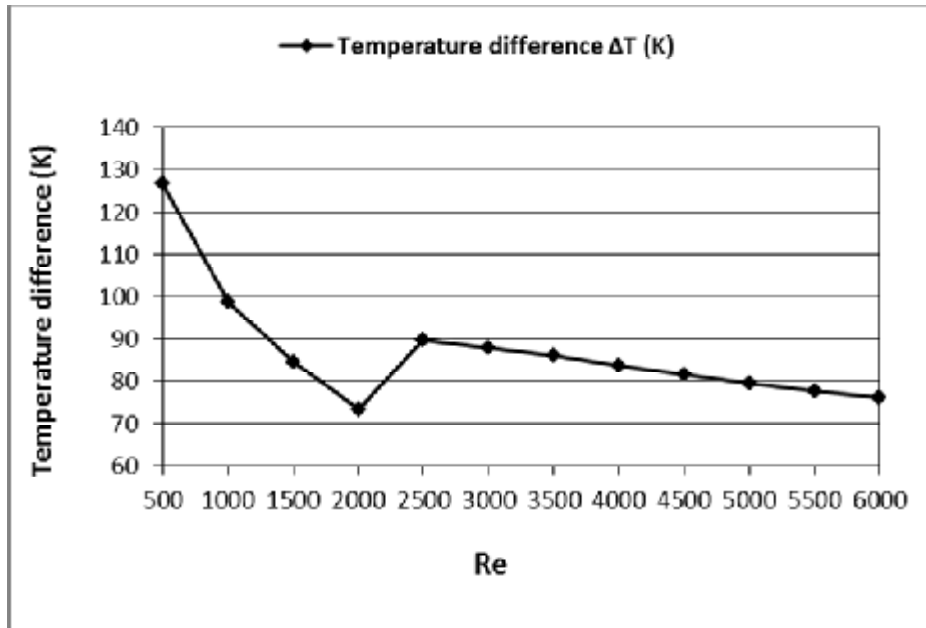
61

Figure 4.31 Inlet and outlet temperature difference with Re for twist annular with water flow

Figure (4.32) shows the relation between heat fluxes from outer tube surface for twist annular with water flow versus Reynolds number. The heat flux is noticed to be variable values and increased with increasing of Reynolds number. It can be shown that the maximum and minimum heat flux values are 333795 W/m^2 and 48035 W/m^2 at Reynolds number of 6000 and 500 respectively.
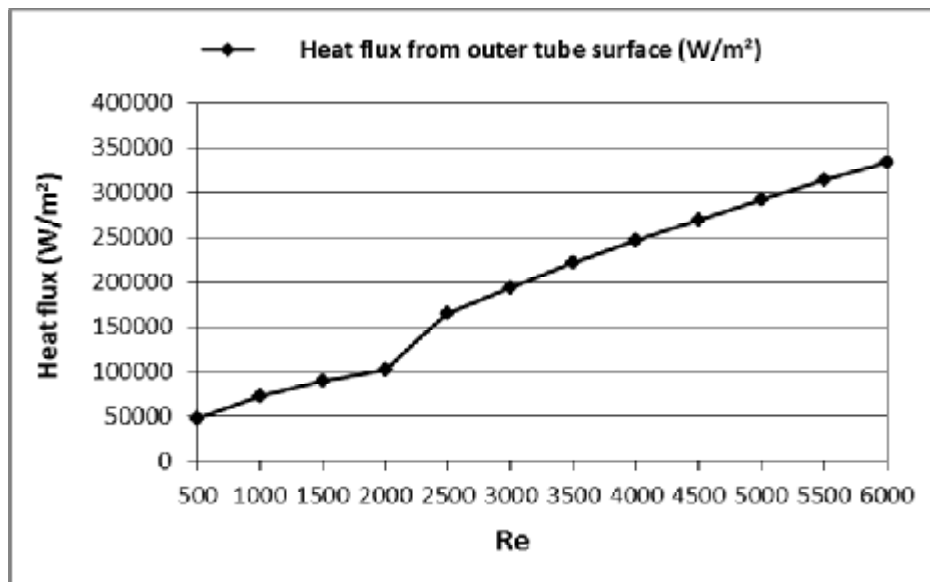

Figure 4.32 Heat flux with Re for twist annular with water flow

Figure (4.33) shows the relation between Nusselt numbers of outer tube surface for twist annular with water flow versus Reynolds number. The Nusselt number is observed to be variable values and increased with increasing of Reynolds number; in the turbulent flow the Nusselt number increased as Reynolds number increased because of increasing in turbulent intensity as Reynolds number increased. It can be shown that the minimum Nusselt number value is 18.4 occurs at Reynolds number of 500 and 127 occurs at Reynolds number of 6000.
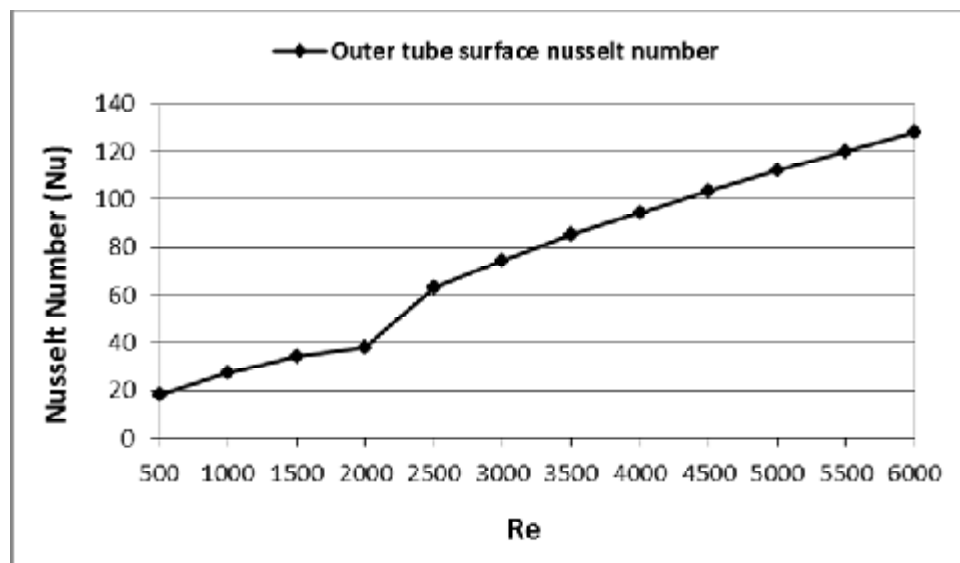

Figure 4.33 Nusselt number with Re for twist annular with water flow

Figure (4.34) shows the relation between film heat transfer coefficients of outer tube surface for twist annular with water flow versus Reynolds number. The factor of heat transfer is seen to be variable values and increased with increasing of Reynolds number. It can be shown that the minimum film heat transfer coefficients value is 552 occurs at Reynolds number of 500 and 3836 occurs at Reynolds number of 6000.
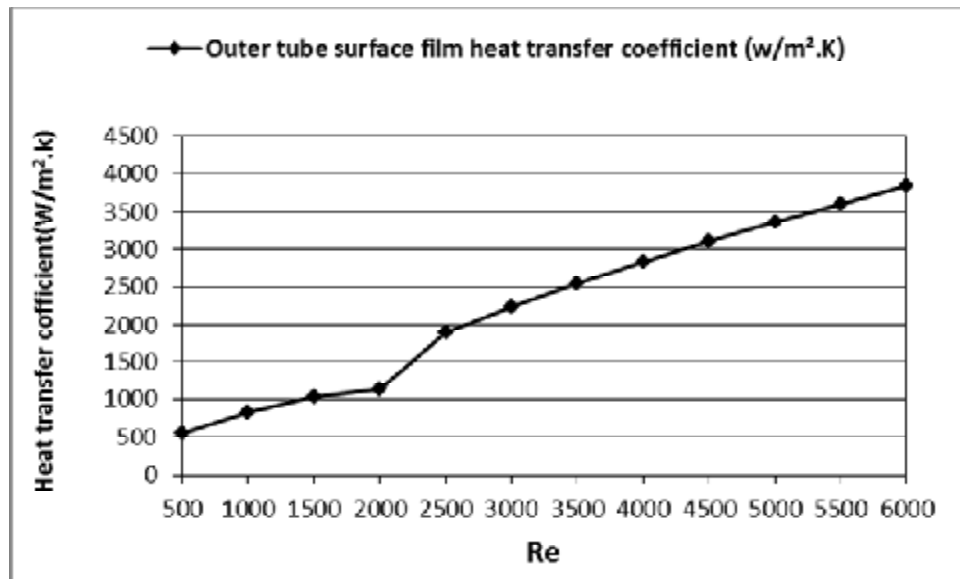
Figure 4.34 Heat transfer coefficient with Re for twist annular with water flow

Figure (4.35) shows the relation between pressure drops in shell side for twist annular with water flow versus Reynolds number. The drop of pressure is noticed to be variable values and increased with increasing of Reynolds number due to increasing in water velocity. It can be shown that the maximum and minimum pressure drop values are 560 Pascal and 15.3 Pascal at Reynolds number of 6000 and 500 respectively.
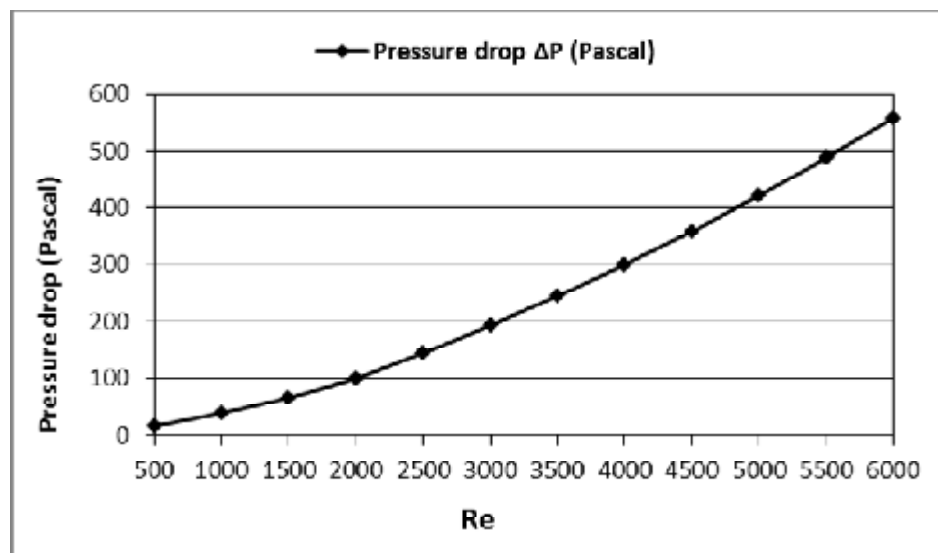

Figure 4.35 Pressure drop with Re for twist annular with water flow

4.6.1 Comparison of Results

Figure (4.36) provides a comparison between the outlet temperatures of air versus Reynolds number in the annular regime for cases of straight and twist annular with air flow. It can be shown that the air outlet temperatures of twist annular increasing by an average of 3.2% compared with air outlet temperatures of straight annular for all Reynolds number, this enhancement in outlet temperature of the twist annular case is occurred due to the additional heat transfer and turbulence produced by the helical flow in the annular regime.
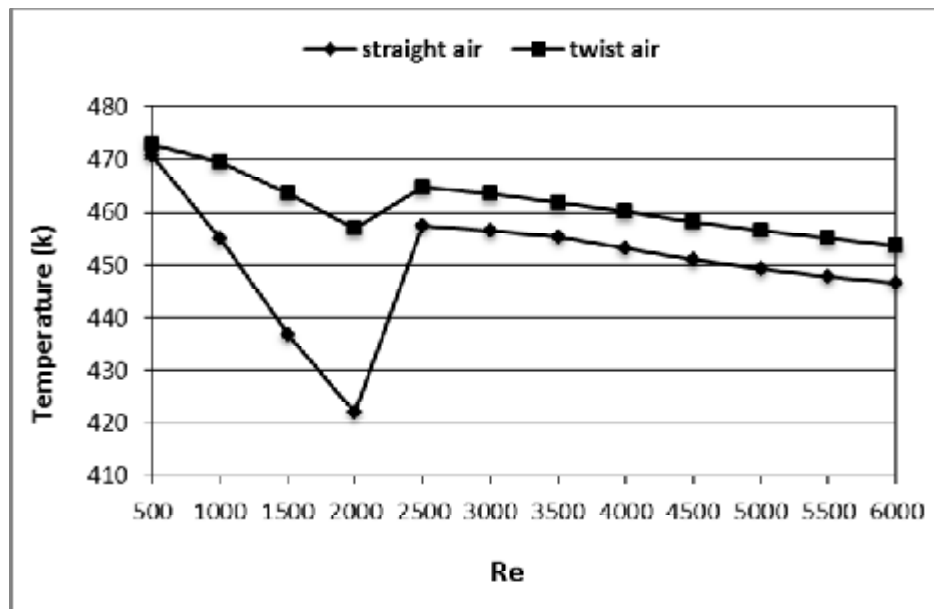

Figure 4.36 Outlet temperatures in the shell side for straight and twist annular with air flow

Figure (4.37) provides a comparison between the outlet temperatures of water versus Reynolds number in the annular regime for cases of straight and twist annular with water flow. It can be shown that the water outlet temperatures of twist annular increasing by an average of 5.8% compared with water outlet temperatures of straight annular for all Reynolds number, this enhancement in outlet temperature of the twist annular case is occurred due to the additional heat transfer and turbulence produced by the helical flow in the annular regime.
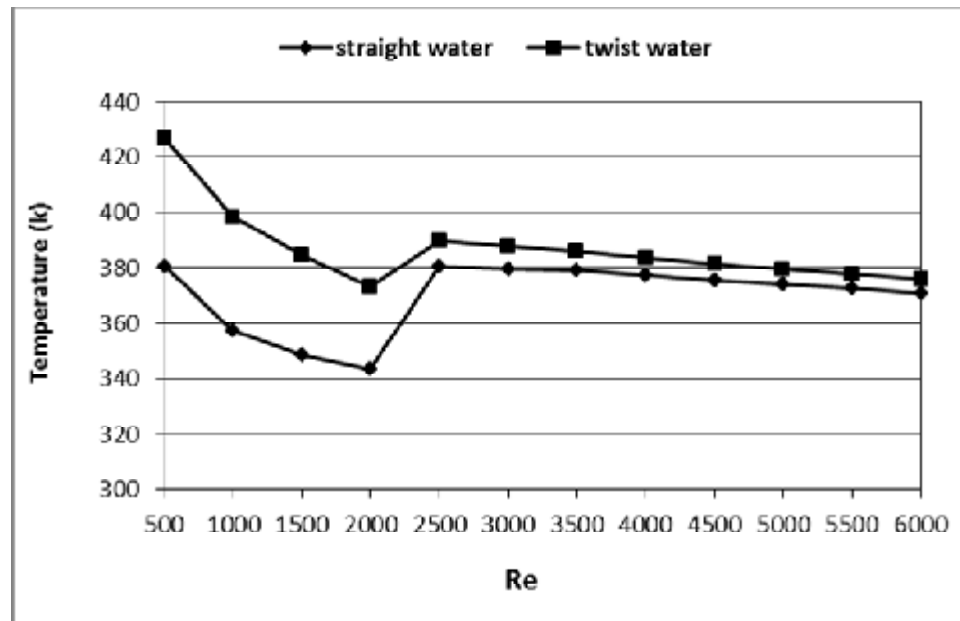
Figure 4.37 Outlet temperatures in the shell side for straight and twist annular with water flow

Figure (4.38) provides a comparison between the temperatures differences of air versus Reynolds number in the annular regime for cases of straight and twist annular with air flow. It can be shown that the air temperatures differences of twist annular increasing by an average of 9.1% compared with air temperatures differences of straight annular for all Reynolds number, this enhancement in temperatures differences of the twist annular case is occurred due to the additional heat transfer and turbulence produced by the helical flow in the annular regime.

Figure 4.38 Temperature difference in the shell side for straight and twist annular with air flow

Figure (4.39) provides a comparison between the temperatures differences of water versus Reynolds number in the annular regime for cases of straight and twist annular with water flow. It can be shown that the water temperatures differences of twist annular increasing by an average of 24.2% compared with water temperatures differences of straight annular for all Reynolds number, this enhancement in temperatures differences of the twist annular case is occurred due to the additional heat transfer and turbulence produced by the helical flow in the annular regime.
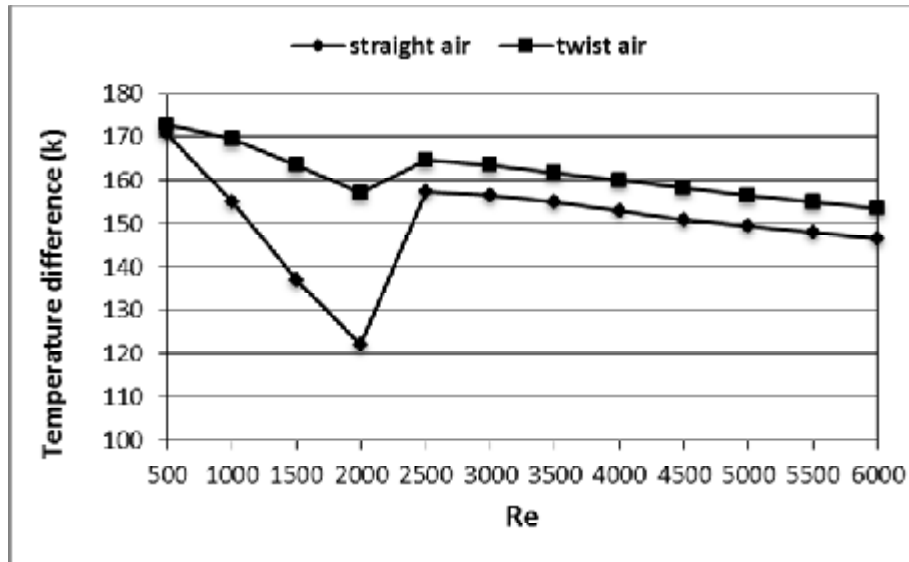
Figure 4.39 Temperature difference in the shell side for straight and twist annular
with water flow

Figure (4.40) provides a comparison between the heat flux from outer tube surface versus Reynolds number in the annular regime for cases of straight and twist annular with air flow. It can be shown that the heat flux of twist annular increasing by an average of 11.2% compared with heat flux of straight annular for all Reynolds number, this enhancement in outlet temperature of the twist annular case is occurred due to the additional heat transfer and turbulence produced by the helical flow in the annular regime.
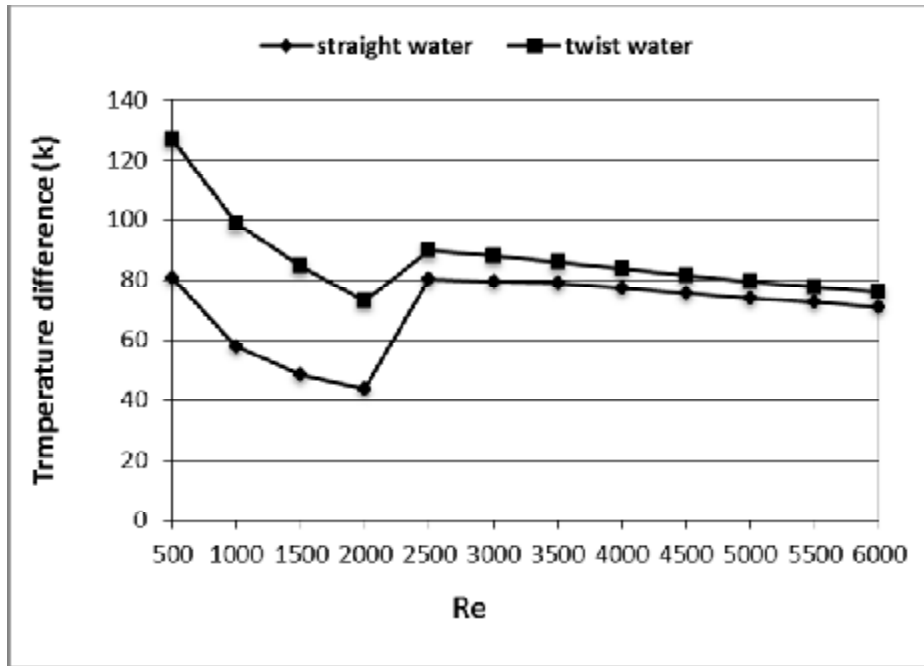
Figure 4.40 Heat flux from outer surface tube for straight and twist annular with air flow

Figure (4.41) provides a comparison between the heat flux from outer tube surface versus Reynolds number in the annular regime for cases of straight and twist annular with water flow. It can be shown that the heat flux of twist annular increasing by an average of 31.3% compared with heat flux of straight annular for all Reynolds number, this enhancement in heat flux of the twist annular case is occurred due to the additional heat transfer and turbulence produced by the helical flow in the annular regime.
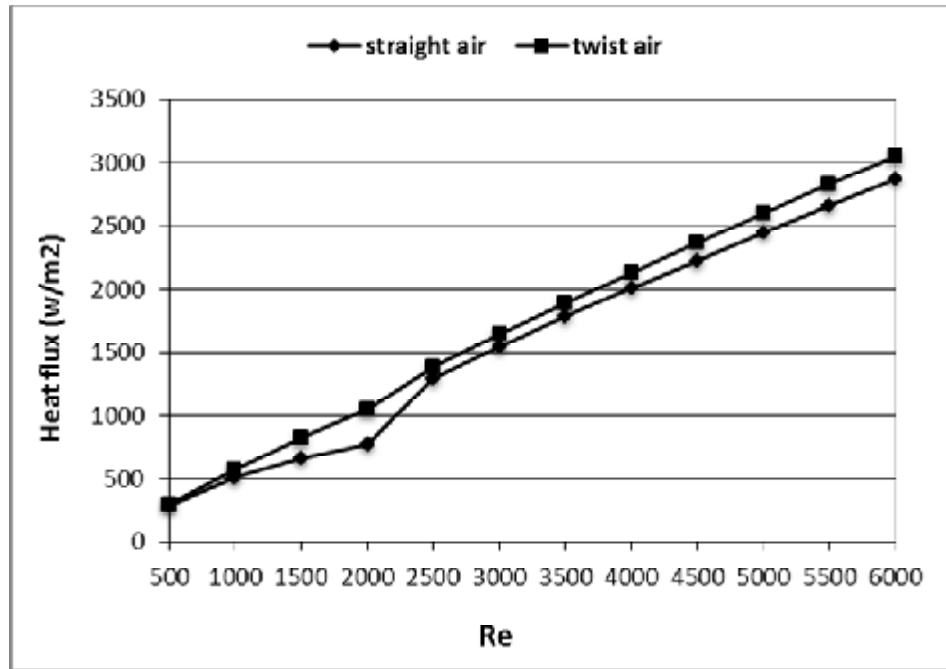
Figure 4.41 Heat flux from outer surface tube for straight and twist annular with water flow

Figure (4.42) provides a comparison between the outer tube surface film factor of heat transfer versus Reynolds number in the annular regime for cases of straight and twist annular with air flow. It is shown that the outer tube surface film heat transfer coefficient of twist annular increasing by an average of 11.2% compared with outer tube surface film heat transfer factor of straight annular for all Reynolds number, this enhancement in outer tube surface film heat transfer coefficient of the twist annular case is occurred due to the additional heat transfer and turbulence produced by the helical flow in the annular regime.
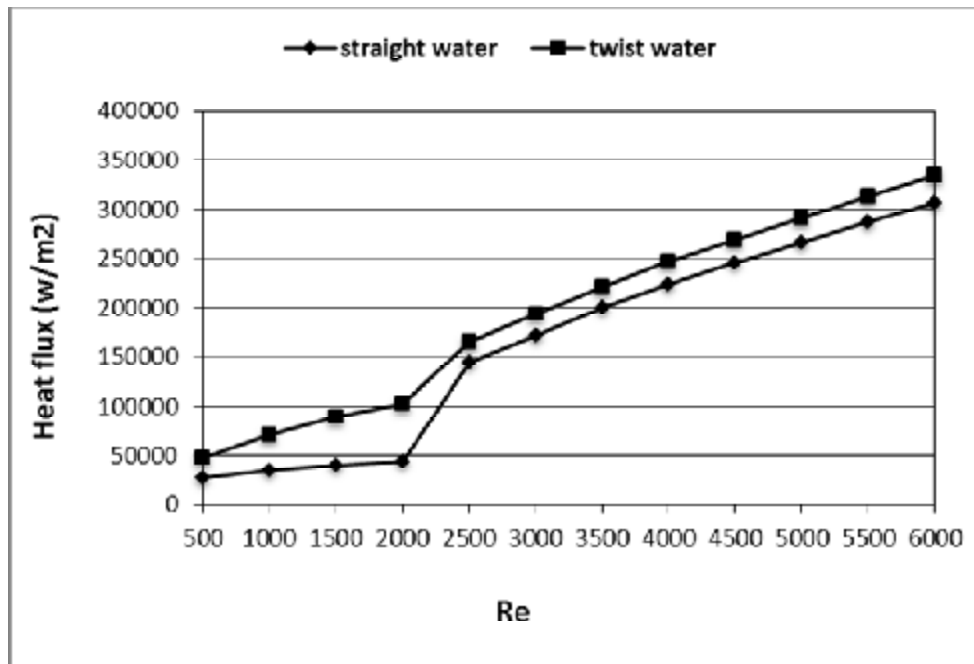
Figure 4.42 Outer tube surface film heat transfer coefficient for straight and twist
annular with air flow

Figure (4.43) provides a comparison between the outer tube surface film factor of heat transfer versus Reynolds number in the annular regime for cases of straight and twist annular with water flow. It can be shown that the outer tube surface film heat transfer coefficient of twist annular increasing by an average of 31.3% compared with outer tube surface film heat transfer factor of straight annular for all Reynolds number, this enhancement in outer tube surface film heat transfer coefficient of the twist annular case is occurred due to the additional heat transfer and turbulence produced by the helical flow in the annular regime.
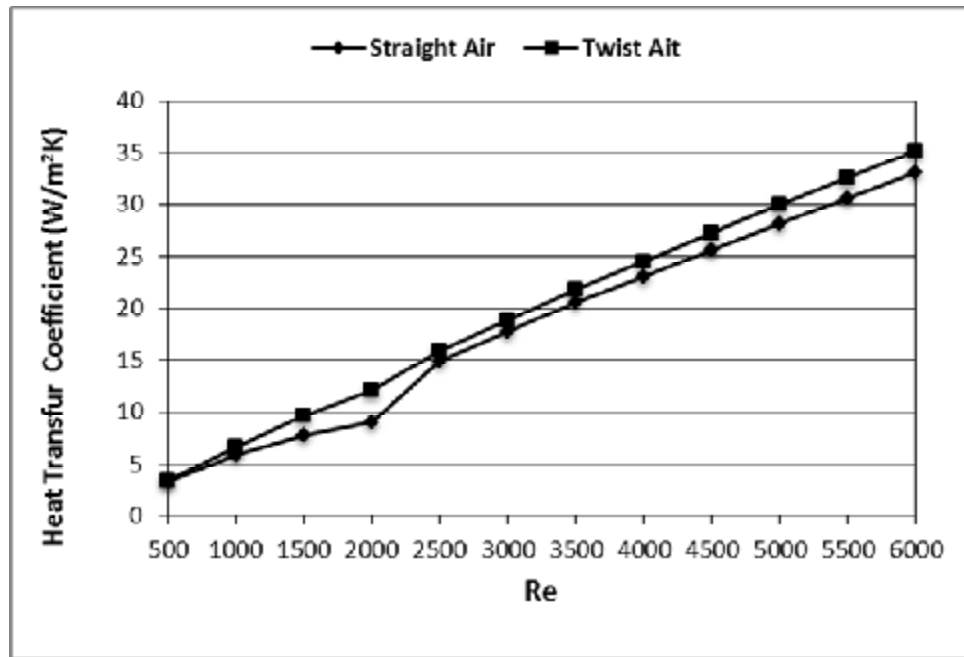
Figure 4.43 Outer tube surface film heat transfer coefficient for straight and twist annular with water flow

Figure (4.44) provides a comparison between the outer tube surface Nusselt number versus Reynolds number in the annular system for cases of straight and twist annular with air flow. It can be shown that the Nusselt number of twist annular increasing by an average of 11.2% compared with Nusselt number of straight annular for all Reynolds number, this enhancement in Nusselt number of the twist annular case is occurred due to the additional heat transfer and turbulence produced by the helical flow in the annular regime.

Figure 4.44 Outer tube surface Nusselt number for straight and twist annular with air flow

Figure (4.45) provides a comparison between the outer tube surface Nusselt number versus Reynolds number in the annular system for cases of straight and twist annular with water flow. It can be shown that the Nusselt number of twist annular increasing by an average of 31.3% compared with Nusselt number of straight annular for all Reynolds number, this enhancement in Nusselt number of the twist annular case is occurred due to the additional heat transfer and turbulence produced by the helical flow in the annular regime.
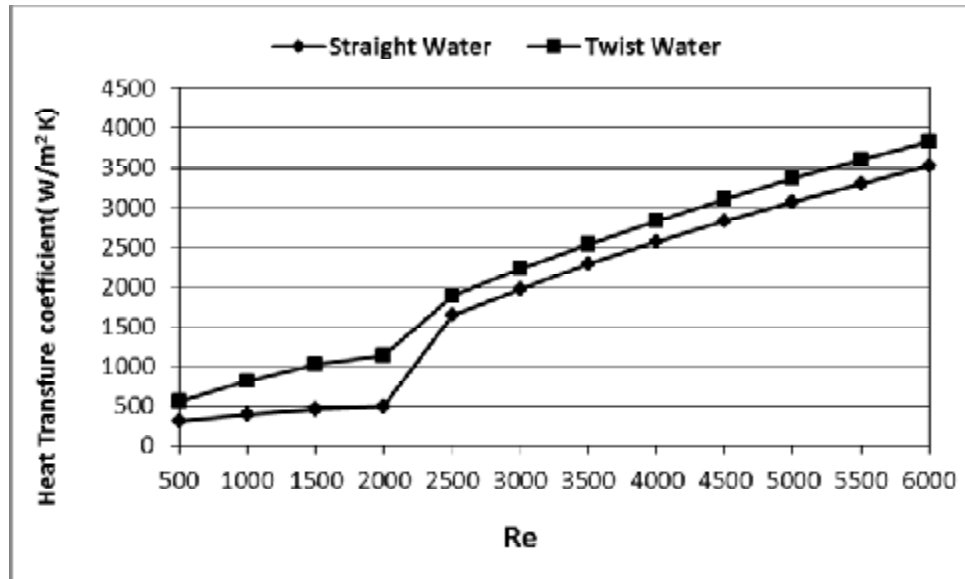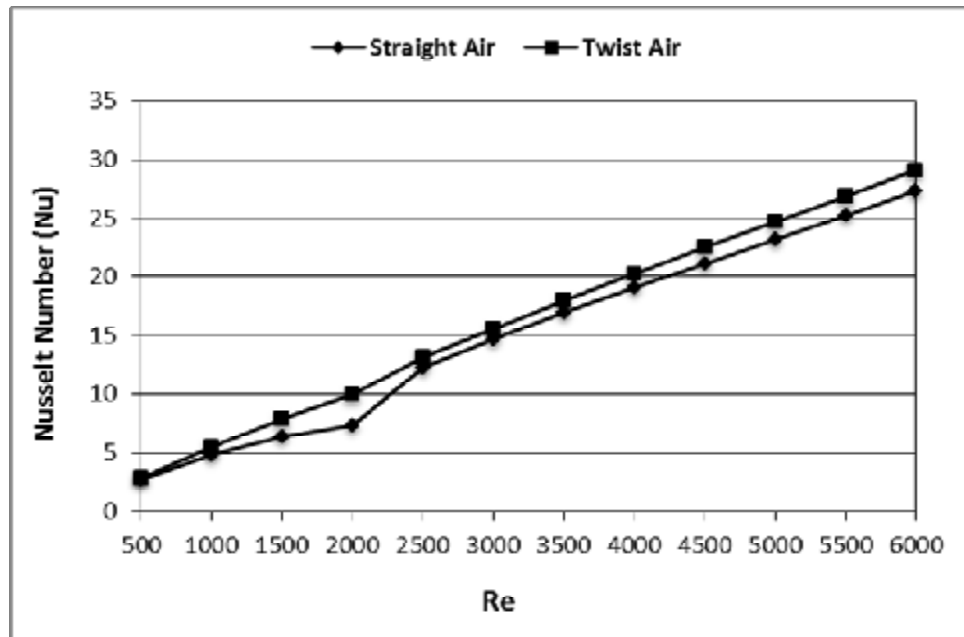
Figure 4.45 Outer tube surface Nusselt number for straight and twist annular with water flow

Figure (4.46) provides a comparison between the pressure drop versus Reynolds number in the annular regime for cases of straight and twist annular with air flow. It can be shown that pressure drop of twist annular increasing by an average of 29% compared with pressure drop of straight annular for all Reynolds number, this enhancement in outlet temperature of the twist annular case is occurred because of the extra flow resistance produced by the helical flow in the annular regime.
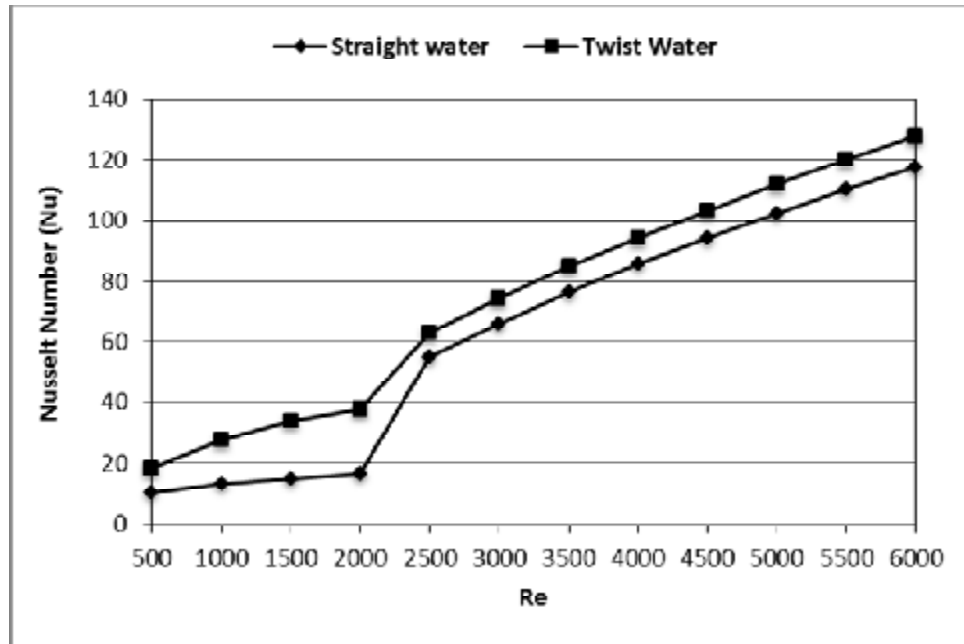
Figure4.46 Pressure drop for straight and twist annular with air flow

Figure (4.47) provides a comparison between the pressure drop versus Reynolds number in the annular regime for cases of straight and twist annular with water flow. It can be shown that pressure drop of twist annular increasing by an average of 29.2% compared with pressure drop of straight annular for all Reynolds number, this enhancement in outlet temperature of the twist annular case is occurred because of the extra flow resistance produced by the helical flow in the annular regime.
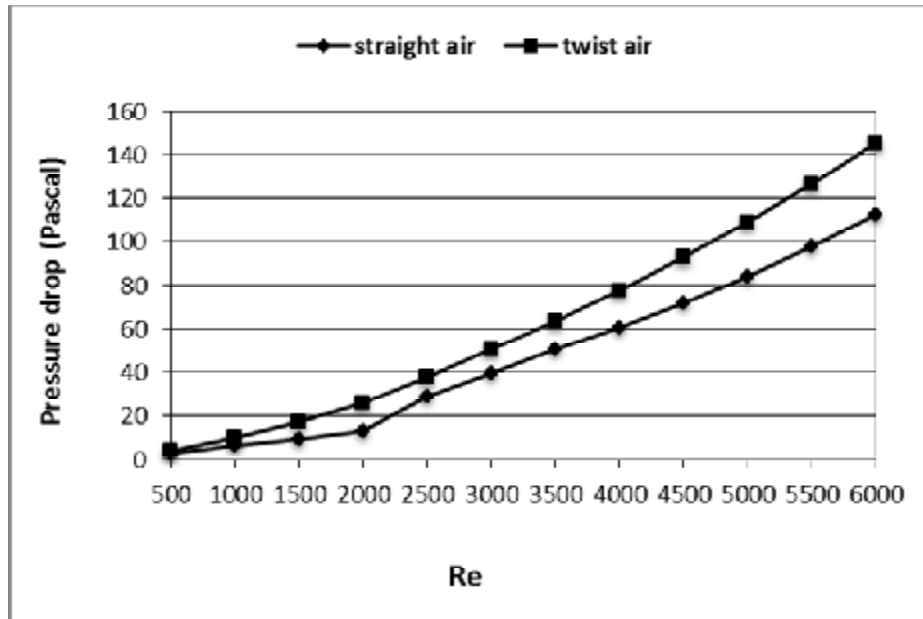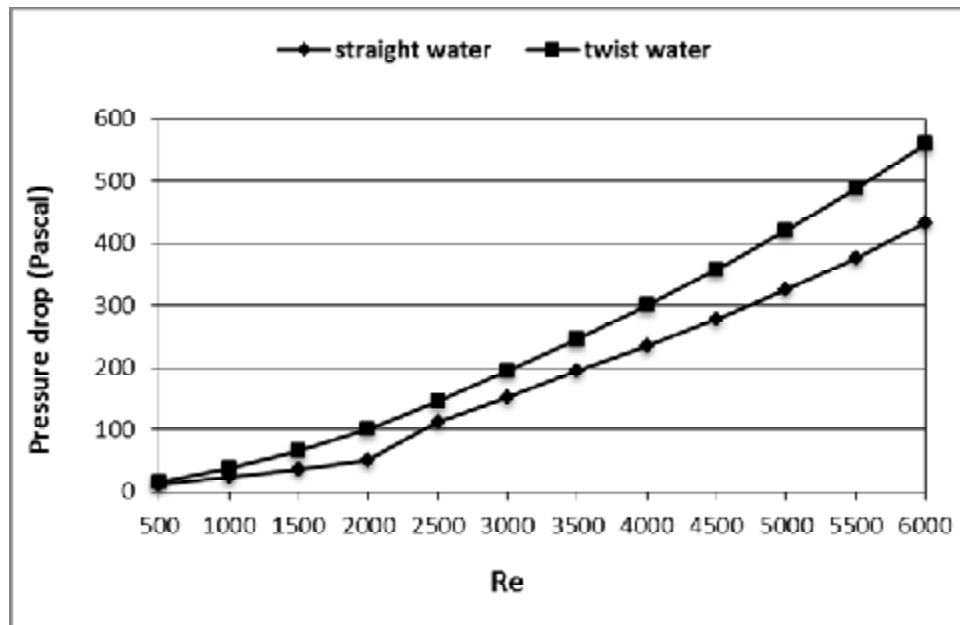

Figure 4.447. Pressure drop for straight and twist annular with water flow

Chapter Five

Conclusion and Recommendations

5.1   Conclusion

A hydrothermal performance of twist annular turbulent flow in a shell and tube heat exchanger has been investigated numerically. The numerical study includes a three dimension numerical solution of four models by a commercial package ANSYS FLUENT 16.0. The boundary conditions of all models that solved by the numerical solution was taken as a constant temperature and constant heat flux for inner tube wall, while the outer wall of shell side was insolation for variable Reynolds number. The following conclusions are detected from this study:

- The annular shape has significant effects on the hydrothermal performance of fluid flow inside the annular regime.
- An enhancement in air and water temperature difference of 9.1 % and 24.2 % respectively for twist annular compared with the straight annular.
- The increasing in air and water outlet temperature of 3.2 % and 5.8 % respectively for twist annular compared with the straight annular.
- The increasing in air and water (heat flux, Nuselts number, and heat transfer coefficient) of 11.2 % and 31.3 % respectively for twist annular compared with the straight annular.
- The increasing in air and water pressure drop of 29 % and 29.2 % respectively for twist annular compared with the straight annular.

5.2   Recommendations

- In spite of the results gained from numerical solution of the present study some future study can be suggested such as:
- The performance of the present shell and tube heat exchanger can be improved to obtain higher outlet air and water temperature by using constant heat flux on the outer shell wall.
- The effect of external fins from outer shell wall may be studied.
- Study the effect of using Nanofluids in the annular regime.

References

[1] Usman Ur Rehman, "Heat Transfer Optimization of Shell-and-Tube Heat Exchanger through CFD Studies", 2011.

[2] R R. K. Shah and D. R Sekulib, " Heat Exchangers".

[3] Chapter 5 Heat Exchangers.

[4] Satyabrata Kanungo, " Numerical Analysis To Optimize The Heat Transfer Rate Of Tube-In-Tube Helical Coil Heat Exchanger", 2014.

[5] Usman Ur Rehman, "Heat Transfer Optimization of Shell-and-Tube Heat Exchanger through CFD Studies", 2011.

[6] Kiran .V.S, Manjunath.H.N, Madhusudhan, "A Study On Optimization Of Low Pressurefeed Water Heater For Thermal Power Plant", 2016.

 [7] A heat exchanger applications general. http://www.engineersedge.com/ heat exchanger/heat_exchanger_application.htm, 2011.

[8] R. K. Shah, "Heat exchangers in encyclopedia of energy technology and the environment", edited by A. Bisio and S. G. Boots, John Wiley & Sons, New York, 1994.

[9] S. Kakac and H. Liu, "Heat exchangers: Selection, rating, and thermal performance"1998.

[10] S.Kanungo "Numerical analysis to optimize the heat transfer rate of tube-in-tuube helical coil heat exchanger".

[11] http://www.wcr-regasketing.com, "Heat exchanger applications." http:// www.wcr-regasketing.com/heat-exchanger-applications.htm, 2010.

[12]A. M. Prithiviraj M, "Shell and tube heat exchangers. part 1: foundation and fluid mechanics, "Heat Transfer, p. 33:799–816., 1998.

[13] A. Barletta, S. Lazzari, Forced and Free Flow in a Vertical Annular Duct Under Nonaxisymmetric Conditions, 606 Vol. 127, JUNE 2005.

[14] Mohamed F. Khalil, Sadek Z. Kassab, Ihab G. Adam, and Mohamed Samaha, "Laminer flow in concentric annulus with a moving core"IWTC12 2008.

[15] S. M. Han,1 Y. J. Kim,2 N. S. Woo,3 and Y. K. Hwang,1, A Study on the Helical Flow of Non-Newtonian Fluids in an Annulus, Osaka, Japan, June 21-26, 2009.

[16] Bendiks Jan Boersma • Wim-Paul Breugem, Numerical Simulation of Turbulent Flow in Concentric Annuli, 2011.

[17] Chungpyo Hong1, Yutaka Asako, Koichi Suzuki, Heat Transfer Characteristics of Gaseous Slip Flow in Concentric Micro-Annular Tubes, JULY 2011.

[18] Ahmed Ali Shaker, A Numerical Study of Low Reynolds Number Incompressible Flow at Entrance and Disturbed Regions Of Concentric Circular Pipes, June 2012.

[19] Stefano Nebuloni1, John R. Thome, Numerical Modeling of the Conjugate Heat Transfer Problem for Annular Laminar Film Condensation in Microchannels, 2012.

[20] L. Maudou, G. H. Choueiri, S. Tavoularis1, An Experimental Study of Mixed Convection in Vertical Open-Ended, Concentric and Eccentric Annular Channels, 2013.

[21] Zhendong Yang Qincheng Bi1, Han Wang, Gang Wu, Richa Hu, Experiment of Heat Transfer to Supercritical Water Flowing in Vertical Annular Channels, 2013.

[22] Wael I. A. Aly1, Computational Fluid Dynamics and Optimization of Flow and Heat Tube-in-Tube Heat Exchangers Transfer in Coiled Under Turbulent Flow Conditions, 2014.

[23] Nicolas Kanaris, Xavier Albets-Chico and Stavros Kassinos, "Numerical simlation of turbulent flow in an eccentric annulus of unit eccentricity", July 3 2015.

[24] N. Kline, S. Tavoularis, An Experimental Study of Forced Heat Convection in Concentric and Eccentric Annular Channels, JANUARY 2016.

[25] Wael I. A. Aly, Thermal and Hydrodynamic Performance of Aqueous CuO and Al2O3 Nanofluids in an Annular Coiled Tube Under Constant Wall Temperature and Laminar Flow Conditions, 2016.

[26] Joon Sang Lee1, Xiaofeng Xu2, Richard H. Pletcher3, "Effects of Wall Rotation on Heat Transfer to Annular Turbulent Flow Outer Wall Rotating", 2005.

[27] José P. B. Mota, António J. S. Rodrigo, "Heat-Transfer Enhancement by Chaotic Advection in the Eccentric Helical Annular Flow", 2008.

[28] Hosny Z. Abou-Ziyan, Abdel Hamid B. Helali, Mohamed Y.E. Selim "Enhancement of forced convection in wide cylindrical annular channel using rotating inner pipe with interrupted helical fins" 2016.

[29] S. Garimella,D.E. Richards, R. N. Christensen, "Experimental Investigation of Heat Transfer in Coiled Annular Duets", 1988.

[30] N. S. Gupte, A. W. Date, "Friction and Heat Transfer Characteristics of Helical Turbulent Air Flow in Annuli", 1989.

[31] ALI M. JAWARNEH, "Heat Transfer Enhancement in Swirl Annulus Flows", 2007.

[32] P. Poskas, V. Simonis, V. Ragaisis, "Heat transfer in helical channels with two-sided heating in gas flow",2011.

[33] Srbislav B. Genic´, Branislav M. Jac´imovic´, Marko S. Jaric´, Nikola J. Budimir, Mirko M. Dobrnjac, "Research on the shell-side thermal performances of heat exchangers with helical tube coils", 2012.

[34] Baiman Chen, Kelvin Ho, Yousif Abdalla Abakr, Andrew Chan, "Fluid dynamics and heat transfer investigations of swirling decaying flow in an annular pipe Part 1: Review, problem description, verification and validation", 2015.

[35] J.Mali, G.Patil, prof . A. R. Acharya, prof . A. T.Pise "Heat transfer enhancement with centrally hollow twisted tape and AL203 water based nanofluid in tubular heat exchanger" 26th June,2016.

[36] Rajesh Bhaskaran, "Introduction to CFD Basics", 2013.

[37] Hamed Sadighi Dizaji*, Samad Jafarmadar, Farokh Mobadersani " Experimental studies on heat transfer and pressure drop characteristics for new arrangements of corrugated tubes in a double pipe heat exchanger" 2015.